REPUBLIC OF TURKEY

YILDIZ TECHNICAL UNIVERSITY

GRADUATE SCHOOL OF SCIENCE AND ENGINEERING

SYNTHESIS AND CHARACTERIZATION OF INHERENTLY ANTIBACTERIAL CATIONIC NANOPARTICLES

Shifa ALHAMVI

MASTER OF SCIENCE THESIS

Department of Bioengineering

Program of Bioengineering

Supervisor

Assoc. Prof. Dr. Murat TOPUZOĞULLARI

January 2023

REPUBLIC OF TURKEY

YILDIZ TECHNICAL UNIVERSITY

GRADUATE SCHOOL OF SCIENCE AND ENGINEERING

SYNTHESIS AND CHARACTERIZATION OF INHERENTLY ANTIBACTERIAL CATIONIC NANOPARTICLES

A thesis submitted by Shifa ALHAMVI in partial fulfillment of the requirements for the degree of **MASTER OF SCIENCE** is approved by the committee on 09.01.2023 in the Department of Bioengineering, Program of Bioengineering.

Assoc. Prof. Dr. Murat
TOPUZOĞULLARI
Yıldız Technical University
Supervisor

Approved By the Examining Committee

Assoc. Prof. Dr. Murat TOPUZOĞULLARI, Supervisor
Yıldız Technical University _____

Assoc. Prof. Dr. Muhammet Übeydullah KAHVECİ, Member
Istanbul Teknik University _____

Assist. Prof. Dr. Yeliz ELALMIŞ, Member
Yıldız Technical University _____

I hereby declare that I have obtained the required legal permissions during data collection and exploitation procedures, that I have made the in-text citations and cited the references properly, that I haven't falsified and/or fabricated research data and results of the study and that I have abided by the principles of the scientific research and ethics during my Thesis Study under the title of Synthesis and Characterization of Inherently Antibacterial Cationic Nanoparticles supervised by my supervisor, Assoc. Prof. Dr. Murat TOPUZOĞULLARI. In the case of a discovery of a false statement, I am to acknowledge any legal consequence.

Shifa ALHAMVI

Signature

This study was supported by both the scholarship from Scientific and Technological Research Council of Turkey (TUBITAK) Grant No: 2210C and the project from the Scientific Research Projects (BAP) Coordination Unit of Yıldız Technical University (Project No: FCD-2022-4900).

Dedicated to my family

and my friends

ACKNOWLEDGEMENTS

First and foremost, I would like to express my deepest gratitude and sincere thanks to my supervisor, Assoc. Prof. Dr. Murat TOPUZOĞULLARI, for providing me with all the help, guidance, support, and encouragement that were invaluable in all the times of researching and writing this study, devoting a great deal of his time, and sharing his great knowledge throughout my study.

I am also grateful to Assoc. Prof. Dr. Tülin ÖZBEK and her doctoral student, lkgül AKMAYAN, for their assistance in carrying out the antibacterial assays for my thesis study. I would like to express my heartfelt gratitude to Assoc. Prof. Dr. Emrah Şefik ABAMOR and his doctoral student Büşra AKGÜL for their contribution and assistance in conducting biological activity tests.

I would like to thank my friends Ala'a MASALMEH, Maria DAABOUL, Samawah HASAN, and Safa AL TAWIL for their motivation, encouragement, and endless support during my thesis work. I would like to extend my thanks to my lab mates, Damla GÖKKAYA, Eda Nur Yetişkin Morkan, and Hatice DEMIR, in addition to the YTU 306-307 Vaccine and Biopolymer Laboratory team and all the people of the Bioengineering Department at Yıldız Technical University, for all their support during my graduate study.

I would also like to give special thanks to my family for their continuous support and understanding when undertaking my study and writing my project. I would not have completed my master's degree without their support and encouragement.

Finally, I would like to thank TÜBİTAK for supporting my study within the scope of the 2210C program (2021/2) Domestic Priority Areas Graduate Scholarship Program during my master's thesis study. And special thanks to the Scientific Research Projects Coordination Unit of Yıldız Technical University for supporting my study with Project No.: FCD-2022-4900.

Shifa ALHAMVİ

TABLE OF CONTENTS

ACKNOWLEDGEMENTS v

TABLE OF CONTENTS vi

LIST OF SYMBOLS viii

LIST OF ABBREVIATIONS ix

LIST OF FIGURES xi

LIST OF TABLES xiii

ABSTRACT xiv

ÖZET xvi

1 INTRODUCTION 1

1.1 Literature Review 1

1.2 Objective of the Thesis 4

1.3 Hypothesis 5

2 GENERAL INFORMATION 6

2.1 Bacterial Infections 6

2.1.1 Gram-Positive and Garam-Negative Bacteria 7

2.1.2 Antibiotics 8

2.1.3 Bacterial Defense Mechanisms 9

2.2 Antibacterial Biomaterials 11

2.2.1 Antibacterial polymers (APs) 11

2.2.2 Antibacterial Nanoparticles 15

3 MATERIALS AND METHOD 23

3.1 Materials 23

3.1 Equipment 24

3.2 Experimental Methods 25

3.2.1 Synthesis of Cationic Poly(4VP-co-OEGMA) Copolymer 26

3.2.2 Synthesis of Polycationic Coated NPs 28

3.2.3 Characterization 29

3.3 In-Vitro Tests 30

3.3.1 Antibacterial Activity Test 30

3.3.2 Biocompatability Test – MTT 32

4 RESULTS AND DISCUSSION 34

4.1 Synthesis and Characterization of Quaternized Poly(4VP-co-OEGMA) Copolymer 34
4.2 Synthesis and Characterization of Polycationic Coated NPs 38
4.3 In-Vitro Tests..... 51
4.3.1 Antibacterial activity assay 51
4.3.2 Biocompatibility test 54
4.4 CONCLUSION 58
REFERENCES 61
PUBLICATIONS FROM THE THESIS 71

LIST OF SYMBOLS

$[I]_0$	Initial Molar of Initiator
$[M]_0$	Initial Molar of Monomer
μm	Micrometer
A	Absorbance
°C	Degree Celsius
cm	Centimetre
Da	Dalton
g	Gram
h	Hour
kDa	Kilo Dalton
L	Liter
M	Molar
mg	Milligram
min	Minutes
mL	Milliliter
M_n	Number Average Molecular Weight
mV	Millivolts
Mw	Molecular Weight
M_w	Molecular weight
nm	Nanometre
µL	Microliter

LIST OF ABBREVIATIONS

4VP	4-Vinylpyridine
ACVA	4-4'azobiscyanoleric acid
Ag	Silver
AMPs	Antimicrobial peptides
APs	Antibacterial Polymers
ATR	Reduced Total Reflectance
BDR	Bacterial Drug Resistance
BIs	Bacterial infections
BrH	1-bromohexane
CB	Concentrations of bound polycations
CU	Concentrations of unbound polycations
Cu	Copper
DBH	1,6-dibromohexane
DLS	Dynamic Light Scattering
DMEM	Dulbecco's Modified Eagle Medium
DMF	Dimethylformamide
DMSO	Dimethyl Sulfoxide
E.coli	*Escherichia coli*
EGDMA	Ethylene glycol dimethacrylate
ELS	Electrophoretic Light Scattering
FT-IR	Fourier Transform Infrared Spectroscopy
Gram (-)	Gram-negative
Gram (+)	Gram-positive
HDPs	Host-Defense Peptides
IACPs	Inherently Antibacterial Cationic Polymers
IC_{50}	Half-maximal inhibitory concentration
MHA	Muller Hilton Agar
MHB	Muller Hilton Broth
MIC	Minimum Inhibition Concentrations
MOI	Multiplicity of infection
NC-NPs	Non-crosslinked NPs
ND	Nanodiamond

NPs	Nanoparticles
OEGMA	Poly (ethylene glycol) methyl ether methacrylate
P4VP	4-vinylpyridine
PAMAMs	Poly(amidoamine)s
PdI	Polydispersity Index
PEI	Polyethylenimine
PLGA	Poly (Lactic-co-Glycolic Acid)
QD	Quaternization Degree
ROS	Reactive Oxygen Species
S.aureus	*Staphylococcus aureus*
SC-NPs	Surface Crosslinked NPs

LIST OF FIGURES

Figure 2.1 Gram-positive and gram-negative bacteria membrane structures.....7
Figure 2.2 Pathogenic bacteria and their related infectious diseases.....8
Figure 2.3 Antibiotic resistance mechanisms.....10
Figure 2.4 Quaternized P4VP chemical structure.....14
Figure 2.5 Antibacterial mechanism action of amphiphilic polycations.....15
Figure 2.6 The antibacterial mechanism of metallic NPs.....18
Figure 3.1 Schematic representation of the experimental method 26
Figure 3.2 Free radical polymerization of poly(4VP-co-OEGMA) copolymer....27
Figure 3.3 Quaternization reaction of poly(4VP-co-OEGMA) copolymer.....27
Figure 4.1 FT-IR spectra of poly(4VP-co-OEGMA) and the quaternized poly(4VP-co-OEGMA) copolymer.....35
Figure 4.2 ^{1}H-NMR Spectrum of poly(4VP-co-OEGMA) copolymer in deuterated DMSO.....36
Figure 4.3 GPC chromatogram of poly(4VP-co-OEGMA) copolymer.....37
Figure 4.4 FT-IR spectrum of PLGA NP.....38
Figure 4.5 Hydrodynamic size distribution of PLGA NPs.....39
Figure 4.6 FT-IR spectra of polycationic NC-NPs.....40
Figure 4.7 FT-IR spectra of PLGA , NC1, and NC8 NPs 41
Figure 4.8 Polycationic NC-NPs' size distribution by %-Intensity 42
Figure 4.9 The hydrodynamic diameter, zeta potentials and polydispersity indices of NC-NPs depending on the concentration of quaternized poly(4VP-co-OEGMA).....43
Figure 4.10 Schematic representation of the number of NPs in the NPs solutions after diluting to equal polycations concentration (1mg/mL).....44
Figure 4.11 Count of NC-NPs diluted to equivalent (1mg/mL) concentration of quaternized poly(4VP-co-OEGMA) depending on the initial concentration of polycation 44
Figure 4.12 SEM images of PLGA NPs(a), NC1-NPs(b) NC3-NPs(c), and NC7-NPs(d) showed spherical morphologies at 20.000X magnification..45
Figure 4.13 FT-IR spectra of polycationic SC-NPs 46
Figure 4.14 Polycationic SC-NPs' size distribution by %-Intensity.....47
Figure 4.15 The hydrodynamic diameter, zeta potentials and polydispersity indices (PDI) of polycationic SC-NPs depending on the concentration of quaternized poly(4VP-co-OEGMA) 48

Figure 4.16 Linear (a), Langmuir (b), and Freundlich (c) adsorption of CN1, CN3, CN5, and CN7 NPs.....50

Figure 4.17 Schematic representation of number of NPs attached to the bacterial surface.....53

Figure 4.18 MOI values as a function of the hydrodynamic diameter of NC-NPs 54

Figure 4.19 Effect of quaternized poly(4VP-co-OEGMA) copolymer, and NC-NPs on L929 fibroblast cell viability.....55

Figure 4.20 Effect of quaternized poly(4VP-co-OEGMA) copolymer, and SC-NPs on L929 fibroblast cell viability.....55

Figure 4.21 Half-maximal inhibitory concentration (IC_{50}) of quaternized poly(4VP-co-OEGMA) copolymer (red dot), NC-NPs (a), and SC-NPs (b) depending on the hydrodynamic diameter of the sample.....57

LIST OF TABLES

Table 3.1 Materials used in the thesis study 23

Table 3.2 Names and brands of devices used in the thesis study.....24

Table 3.3 Codes and concentrations of non-crosslinked NPs (NC-NPs) and surface crosslinked polycationic NPs (SC-NPs).....28

Table 4.1 Hydrodynamic diameters (D), polydispersity index (PdI), zeta potentials (ζ_P), quaternization degrees (QD), and counts of NPs.....49

Table 4.2 MIC values of quaternized poly(4VP-co-OEGMA), NC-NPs, and SC-NPs 52

Table 4.3 MOI values of NC-NPs.....53

Table 4.4 IC_{50} values of quaternized poly(4VP-co-OEGMA) copolymer, NC-NPs, and SC-NPs in the group on L929 fibroblast cells.....56

ABSTRACT

Synthesis and Characterization of Inherently Antibacterial Cationic Nanoparticles

Shifa ALHAMVI

Department of Bioengineering

Master of Science Thesis

Supervisor: Assoc. Prof. Dr. Murat TOPUZOĞULLARI

Bacterial infectious-associated diseases rank among the most common causes of death worldwide. Owing to excessive antibiotic usage and frequent therapeutic switching, bacterial resistance has grown to be a serious challenge in treating bacterial infections. Therefore, new antibacterial materials are required to improve bacterial selectivity, reduce antibiotic resistance, and overcome the issues of existing antibacterial agents.

Cationic nanoparticles have attracted considerable interest due to their inherent antibacterial activity without the need for an antibacterial agent and their direct contact with the bacterial cell wall without penetrating the cell, which makes them less likely to be exposed to most antibiotic-resistance mechanisms. Positively charged quaternized poly(4-vinylpyridine) (P4VP) can be used to produce polymeric cationic nanoparticles that are inherently antibacterial and can be used in a wide range of biomedical applications.

In this study, polymeric cationic nanoparticles were produced by coating PLGA nanoparticles with cationic copolymers of 4-vinylpyridine (4VP) and oligo (ethylene glycol) methyl ether methacrylate (OEGMA) to obtain inherently

antibacterial nanoparticles. The cationic copolymers on the surface of the nanoparticles were further crosslinked. The produced copolymer and nanoparticles were characterized with NMR, FT-IR, DLS, ELS spectroscopies, GPC, and SEM. Finally, the antibacterial activity and cytotoxicity of the produced nanoparticles were investigated.

After coating the PLGA nanoparticle with different concentrations of quaternized poly(4VP-co-OEGMA) copolymer, cationic nanoparticles with hydrodynamic diameters ranging between 130 and 415 nm, polydispersity indices below 0.3, and zeta potential values greater than +40 mV were obtained. The produced nanoparticles exhibited antibacterial activity against both S. aureus and E. coli in microdilution assays. In addition, the produced materials were biocompatible with L929 fibroblasts at concentrations above their minimum inhibitory concentrations (MIC). The produced inherently antibacterial cationic nanoparticles have the potential to be used in biomedical applications such as drug delivery systems, surface coatings, and wound dressings.

Keywords: 4-vinylpyridine, antibacterial, nanoparticles, polycations, quaternization.

ÖZET

Kendiliğinden Antibakteriyel Katyonik Nanopartiküllerin Sentezi ve Karakterizasyonu

Shifa ALHAMVI

Biyomühendislik Anabilim Dalı

Yüksek Lisans Tezi

Danışman: Doç. Dr. Murat TOPUZOĞULLARI

Bakteriyel enfeksiyöz ilişkili hastalıklar, dünya çapında en yaygın ölüm nedenleri arasında yer almaktadır. Aşırı antibiyotik kullanımı ve tedavilerde farklı ilaçların sık kullanımı nedeniyle, bakteriyel direnç, bakteriyel enfeksiyonların tedavisinde ciddi bir sorun haline gelmiştir. Bu nedenle, bakteriyel seçiciliği artırmak, antibiyotik direncini azaltmak ve mevcut antibakteriyel ajanlardan kaynaklı sorunlarının üstesinden gelmek için yeni antibakteriyel malzemelerin geliştirilmesi gerekmektedir.

Katyonik nanopartiküller, farklı bir antibakteriyel ajana ihtiyaç duymaksızın kendilliğiden antibakteriyel aktiviteleri ve hücreye nüfuz etmeden bakteri hücre duvarı ile doğrudan temas etmeleri nedeniyle büyük ilgi çekmiştir; bu da onların çoğu antibiyotik direnç mekanizmasına maruz kalma olasılıklarını azaltmakta ve bakteriyel enfeksiyonları tedavi etmek için kullanılma olasılıklarını artırmaktadır. Polimerik katyonik nanopartiküller, pozitif yüklü kuaternize poli(4-vinilpiridin) (P4VP)'den üretilerek kendiliğinden antibakteriyel nanopartiküller elde edilebilmektedir ve birçok biyomedikal uygulamada kullanılabilmektedirler.

Bu çalışmada, kendiliğinden antibakteriyel nanopartiküller elde etmek için PLGA nanopartiküllerin 4-vinilpiridin (4VP) ve oligo (etilen glikol) metil eter metakrilat (OEGMA) katyonik kopolimerler ile kaplanmasıyla polimerik katyonik nanopartiküller üretilmiştir. Nanopartiküllerın yüzeyindeki katyonik kopolimerler ayrıca çapraz bağlanmıştır. Üretilen kopolimer ve nanopartiküller NMR, FT-IR, DLS, ELS spektroskopileri, GPC ve SEM ile karakterize edilmiştir. Son olarak, üretilen nanopartiküllerin antibakteriyel aktivitesi ve sitotoksisitesi incelenmiştir.

Sonuçlar, PLGA nanopartikül farklı konsantrasyonlarda kuaternize poli(4VP-ko-OEGMA) kopolimer ile kaplandıktan sonra hidrodinamik çapları 130 ile 415 nm arasında, polidispersite indisi 0,3'in altında ve zeta potansiyel değerleri +40 mV 'dan fazla olan katyonik nanopartiküller elde edilmiştir. Üretilen nanopartiküller, mikrodilüsyon testlerinde hem *S. aureus* hem de *E. coli* bakterilere karşı antibakteriyel aktivite göstermiştir. Ayrıca, üretilen malzemeler, minimum inhibitör konsantrasyonlarının (MIC) üzerindeki konsantrasyonlarda L929 fibroblast üzerinde biyouyumludur. Üretilen kendiliğinden antibakteriyel katyonik nanopartiküller, ilaç salım sistemleri, yüzey kaplamaları ve yara örtüsü gibi biyomedikal uygulamalarda kullanılma potansiyeline sahıplerdır.

Anahtar Kelimeler: 4-vinilpiridin, antibakteriyel, nanopartiküller, polikatyonlar, kuaternizasyon.

1
INTRODUCTION

1.1 Literature Review

Several health issues result from bacteria due to their ability to invade tissues, release toxins, or trigger inflammation that may cause serious diseases such as catheter-associated [1], heart, nervous system, gastrointestinal tract, or lung infections, and it may increase the risk of cancer [2] [3]. Furthermore, in some cases, bacterial infections (BIs) are among the serious problems in biomedical devices and implants leading to the failure of implants, and increasing the probability of repeating the surgery [4]. Therefore, since the early 1800s, BIs were considered to be one of the most common causes of death in the world [5] [4]. Most BIs are caused by gram-negative and gram-positive bacteria, such as *Escherichia coli* (*E.coli*) and *Staphylococcus aureus* (*S.aureus*) respectively [1].

Antibiotics have been used to treat BIs such as cephalosporins, ciprofloxacin, penicillins, and vancomycin [1] [6]. Owing to the widespread overuse of antibiotics without appropriate medical indications, inappropriate selection of alternative antibacterial, and frequent switching between antibacterial treatments, bacteria developed multi-drug resistance to antibacterial agents [6] [7]. Which, in turn, made antibiotics ineffective against BIs, led to high BIs' mortality rates [5]. As well as antibacterial multidrug resistance, bacteria have different ways to defend themselves against antibacterial agents, such as by forming biofilms, capsules, and producing spores [3].

Therefore, new alternative antibacterial biomaterials have been developed to be used in the treatment of BIs that are different from the mechanisms of antibiotics, such as antibacterial agent-based or inherently antibacterial biomaterials [4].

Nowadays, cationic polymeric antibacterial biomaterials get considerable interest due to their various advantages, such as showing antibacterial properties without the need for additional antibacterial agents, being biocompatible, having long-

term activity, chemical stability, and ease of production and modification [8]. In addition, they are less likely to produce bacterial drug resistance (BDR) [8].

In this context, nanotechnology provides novel physiochemically modified polymeric nanomaterials with superior antibacterial features to be more effective than their bulk forms and improve their ability to address the multi-drug resistance [9]. As a result, recent literatures have focused on biomaterials based on inherently cationic polymeric nanoparticles (NPs) as an alternative strategy for combating bacterial diseases, which are less likely to increase bacterial resistance due to direct contact and interaction with the bacterial cell wall without the need for cell penetration [10]. Furthermore, NPs with multiple functions can be targeted to a particular strain of bacteria or an infectious tissue and hold great promise as a treatment for multidrug resistance in bacteria [11]. NPs reduce the negative effects of traditional antibiotics and increase their antibacterial activity [11]. Moreover, due to their excellent antibacterial activity on several gram-positive and gram-negative bacteria, they are effective for use in many bioapplication areas, such as wound dressings, medical devices, and implants [12].

Cationic polymeric NPs can be produced by different techniques and from diverse polymeric structures [13] [14]. Emulsion polymerization [14], nanoprecipitation [14], coating the NP surface [13], or micellization [15] are some of the techniques to prepare polymeric NPs, while homopolymers [16], copolymers [16], or monomers [17] are the main materials used in these preparation techniques [16].

Kadayifci et al. produced a block copolymer from 4-vinylpyridine (4VP) and oligoethyleneglycol methyl ether methacrylate (OEGMA) monomers. The produced poly(4VP-b-OEGMA) amphiphilic block copolymer was core crosslinked using a bifunctional alkylating agent by a quaternization reaction after micellization, resulting in inherently antibacterial cationic crosslinked polymeric materials [15]. Quaternary ammonium groups were located in the core of this system, not on the surface. It showed long-term stability with activity against gram-negative bacteria [15].

In another study, Ozay et al. synthesized polymeric 4VP-NPs via an oil-in-water microemulsion using ethylene glycol dimethacrylate (EGDMA) as a crosslinker. They quaternized the pyridine rings in the NPs to obtain positively charged NPs. In addition, they produced an antibacterial NP by adding silver and copper ions to these NPs [11]. The synthesized positively charged NPs suggest that they can be used to inhibit bacterial growth for various gram-positive and gram-negative bacteria and can be applied to various surfaces as a filler with other materials [11].

Cao et al., on the other hand, produced N-alkylated P4VP-functionalized nanodiamonds (NP4VP ND) by covalently binding the surface of ND with quaternized P4VP to provide antibacterial properties as well as to solve the problems of agglomeration and poor dispersion stability of ND [18]. They found that NP4VP-functionalized NDs had good antibacterial activity, compared to unmodified ND, against both *E. coli* and *S. aureus*.

It is revealed that polycationic NPs are used in different antibacterial application areas, such as catheters. Francesko et al. [19], improved the silicone urinary catheters by constructing layer-by-layer surface coatings of both the polyanion hyaluronic acid (HA) and the polycationic aminocellulose nanospheres (ACNSs) in order to prevent the formation of biofilms and minimize the likelihood of BDR. ACNSs multilayers were 40% more antibacterial than bulk conjugate (AC) coatings. This resulted in improved inhibition of the *Pseudomonas aeruginosa* biofilm. In the absence of bacteria, the coatings were durable. However, the biofilm was eradicated due to the disassembly during the *Pseudomonas aeruginosa* incubation followed by the release of the polycationic ACNSs. In comparison to the 10 bilayers of AC required to inhibit biofilm growth, 5 bilayers of HA/ACNSs were enough to inhibit its growth [19].

Moreover, another application is in dental composites production, Beyth et al. [20], produced crosslinked quaternized poly(ethyleneimine) NPs (PEI NPs) which were embedded within three different types of dental composite resins: bonding, flowable, and hybrid. The antibacterial activity of these materials against Streptococcus mutants revealed a significant antibacterial effect when 1% of PEI

NPs were embedded within them. Furthermore, for a month, composite resins containing PEI NPs maintained antibacterial activities without leaching or affecting their mechanical properties. In composite resin restorations, antibacterial NPs may help to reduce biofilm and the likelihood of subsequent caries [20].

Antibacterial activities are also increased by coating poly (Lactic-co-Glycolic Acid) (PLGA) NPs with chitosan (CS). It has been shown in studies that the antibacterial properties of PLGA NPs loaded with an antibiotic, Ciproflaxin, are significantly increased because of coating the surface with CS. This new system, compared with uncoated PLGA NPs, showed controlled drug release, increased encapsulation efficiency, and a larger inhibitory zone [21]. However, PLGA NPs coated with polycations as inherently antibacterial materials had not been reported previously in the literature.

In this study, a quaternized poly(4VP-co-OEGMA) copolymer was used for coating PLGA NPs to produce differently sized cationic polymeric NPs with inherent antibacterial properties for the first time. With this study, the surface of PLGA NP has been coated with different amounts of positively charged copolymer, and the produced inherently antibacterial NPs do not release any drug.

1.2 Objective of the Thesis

The study aimed to produce differently sized inherently antibacterial cationic polymeric NPs by coating the PLGA NPs with quaternized poly(4VP-co-OEGMA) copolymers. The effect of NP size and copolymer concentration on the antibacterial activities of produced NPs were investigated against gram-positive and gram-negative bacteria.

For this purpose, the major steps given below were followed:

- Synthesis and characterization of antibacterial quaternized poly(4VP-co-OEGMA) copolymers,
- Production of differently sized NPs by coating PLGA NPs with quaternized poly(4VP-co-OEGMA) copolymers,

- Investigation of the antibacterial activity and biocompatibility of all the materials produced.

1.3 Hypothesis

Antibacterial cationic nanoparticles can be produced by different methods, such as micellization of block copolymers, emulsion polymerization, dendrimer synthesis, etc. The surface coating of non-antibacterial nanoparticles with antibacterial cationic polymers is another method to prepare such antibacterial nanoparticles. In this thesis, PLGA nanoparticles were coated with the inherently antibacterial copolymer of poly(4VP-co-OEGMA). It was hypothesized that using different amounts of copolymer in the coating of PLGA nanoparticles would form different sizes of antibacterial NPs and that the antibacterial activity of the produced coated nanoparticles would depend on their size. The evaluation of size dependence in the antibacterial activity of polymeric nanoparticles would allow for the preparation of more efficient nanostructures for antibacterial applications.

2
GENERAL INFORMATION

2.1 Bacterial Infections

Infectious-associated diseases rank among the most common causes of death worldwide [5]. Infections are caused by microorganisms such as fungi, protozoa, algae, viruses, archaea, or bacteria [22]. Bacteria are prokaryotes that have a simple cellular structure compared to eukaryotes [23]. They consist of cytoplasm, DNA, ribosomes, and the plasma membrane; however, they do not have nuclei and some organelles like mitochondria, the Golgi apparatus, and the endoplasmic reticulum. In some species capsules, flagellum, or pili can be also a part of their structure [23].

Bacteria are important to the earth's ecosystems and can be found everywhere, even in the human body [23]. Just little number of bacteria can cause diseases called pathogenic bacteria [23]. Although they are few, several beneficial or harmless bacteria can transform into pathogenic forms if they grow in abnormal conditions, causing bacterial infections (BIs) [3]. Pathogenic bacteria have the ability to invade tissues, release toxins, or trigger inflammation, causing serious diseases called bacterial infection-associated diseases such as Tuberculosis, pneumonia, meningitis, gonorrhea, and cholera [2] [3]. BIs have high morbidity and mortality rates; therefore, they have recently been considered one of the most serious and widespread health concerns worldwide [4].

Bacteria are classified according to their shape, gram-staining, genotype, and growth characteristics [3]. Also, their associated diseases can be classified according to the same classification [3].
For example, according to their:

- morphology: spirochete infections,
- gram-staining: gram-negative and gram-positive infections,

- growth characteristic: aerobic and anaerobic infections [3].

2.1.1 Gram-Positive and Garam-Negative Bacteria

Bacilli and cocci, both gram-positive and gram-negative, were the first pathogens identified [23]. Under a light microscope, bacteria can be dyed either red for gram-negative bacteria or violet for gram-positive bacteria because of the distinction in their cell walls, especially both the difference in peptidoglycan layer thickness and the outer lipid membrane layer presence [23]. The differing visualization features between these two types is important for a successful clinical diagnosis, since finding out the ethology is the first and the most important step of right treatment [24].

As shown in Figure 2.1, the major differences between these two types are that the gram-positive bacteria, often known as monoderms, have a thick and rigid structure consisting of a multiple peptidoglycan cell wall layer with the absence of the outer lipid membrane layer [25]. On contrast, gram-negative bacteria, or diderms, have a thin structure consisting of a thin peptidoglycan layer with the presence of an outer lipid bilayer membrane [26]. Furthermore, unlike the gram-negative bacterial cell wall, the gram-positive bacterial cell wall has teichoic acids [25] [26].

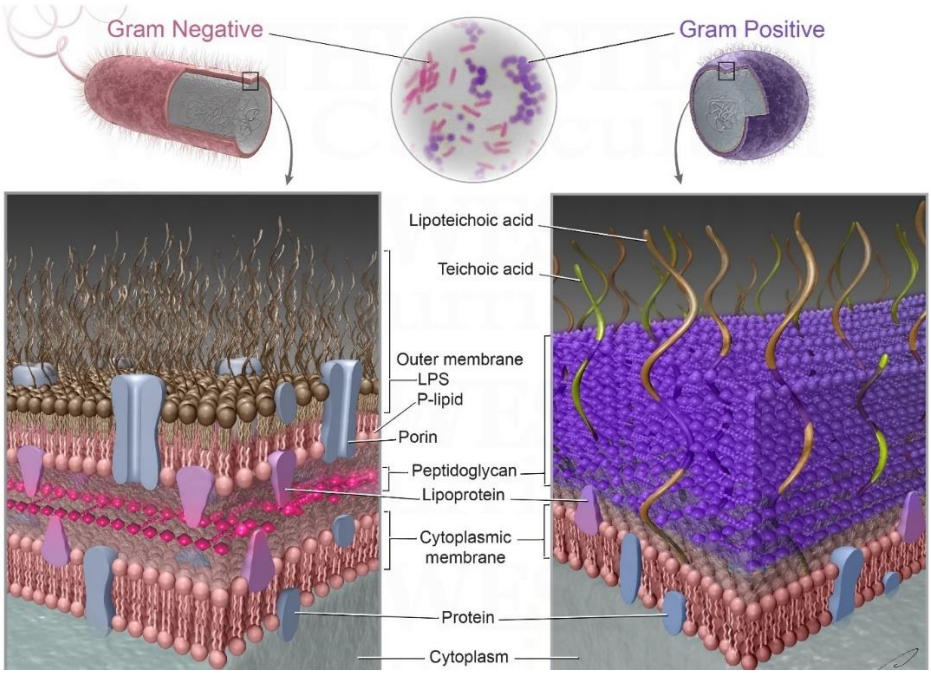


Figure 2.1 Gram-positive and gram-negative bacteria membrane structures [27]

E.coli and *S.aureus* are examples of gram-negative and gram-positive bacteria, respectively [23]. Moreover, they each result in distinct infections, which can be treated with different antibiotics [23]. They cause different types of infections, such as skin and soft tissue infections, surgical site infections, bloodstream infections, infections of the central nervous system, pulmonary infections, osteoarticular infections, prosthetic joint infections, and intravascular catheter infections [23]. Furthermore, in some cases, BIs are among the most serious problems in biomedical devices and implants leading to the failure of implants and increasing the probability of repeating the surgery [4]. Figure.2.2. shows some of gram-positive, gram-negative bacteria and their related infectious diseases:

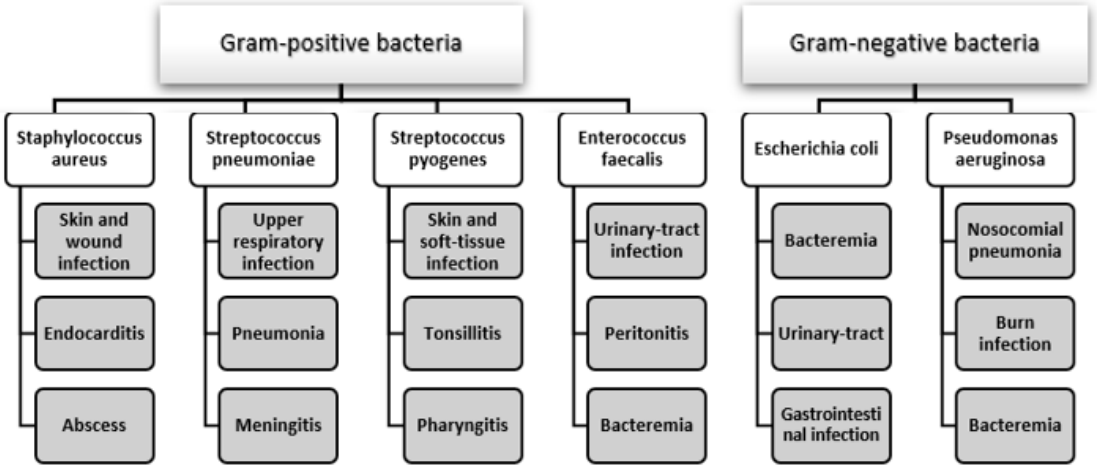


Figure 2.2 Pathogenic bacteria and their related infectious diseases [28]

2.1.2 Antibiotics

To kill or inhibit the growth of germs, antibacterial agents, often known as antibiotics, have been used, such as cephalosporins, ciprofloxacin, penicillins, and vancomycin [6] [14]. They were the most popular therapeutic agents due to their affordable cost and highly effective treatment for BIs [10]. Antibiotics are highly effective against most bacteria because they target their major metabolic processes, including bacterial cell wall formation, protein synthesis, RNA translation, and DNA replication machinery [10] [29]. However, antibiotic overuse has resulted in bacteria developing different defense mechanisms to reduce and limit the efficacy of these agents [30].

2.1.3 Bacterial Defense Mechanisms

Several bacterial processes, including colonization and invasion of mucosae, endocytosis, phagocytosis, adherence to cell membranes, etc., can modulate the interactions between bacteria and target cells, preventing the activation of adaptive and innate systems and allowing bacteria to live in harsh conditions [30]. In addition to the bacterial gene alterations that resulted in drug resistance against antibiotics, bacteria defend themselves by different mechanisms [31], which are represented by adhesion factors, bacterial carbohydrate capsules, biofilms, antiphagocytic factors, toxins, deoxyribonucleases, proteases, lytic agents, lipases, etc [30].

- **Antibiotic Resistance**

The ability of bacteria to resist antibiotics, called antibiotic resistance, results from random changes in bacterial genes that are one of the bacteria's defense mechanisms against antibiotics [30] [31].

Due to the extensive use of antibiotics and the frequent switching of antibacterial treatments, bacterial resistance has grown to be a significant health issue [32]. Drug-resistant and multidrug-resistant of bacteria are the results of the interaction of several intrinsic and extrinsic factors [32].

These resistance factors can be described in four ways (Figure 2.3): antibiotics may inactivate some vital bacterial enzymes [31], alter antibiotic binding sites [30], change the metabolic pathways [31], and reduce the antibiotic density in bacteria by decreasing both their membrane permeability and their efflux through membrane pumps [30] [31]. As a consequence, the rise of antibiotic resistance has reduced the efficacy of many antibiotics [6].

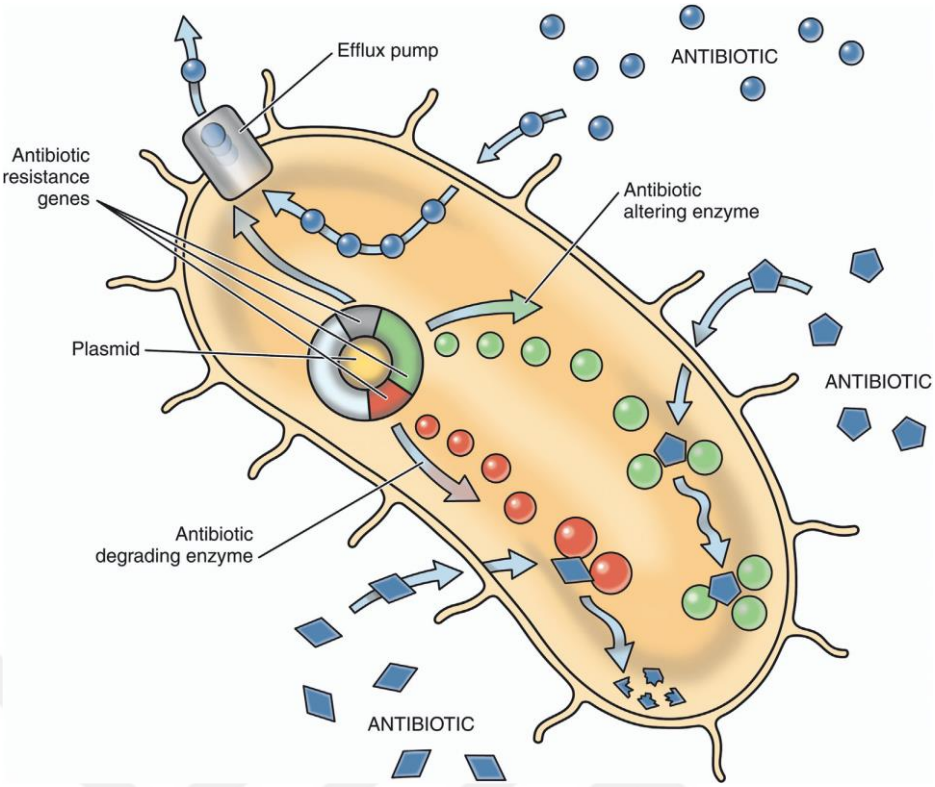


Figure 2.3 Antibiotic resistance mechanisms [30]

- **Biofilm**

Bacterial colonization occurs when bacterial virulence processes build up a cluster of connected bacteria in a self-produced polymeric matrix made up of proteins, polysaccharides, and DNA, called a biofilm matrix, on the membrane surface [33] [30]. Bacteria inside biofilm are resistant to macrophage phagocytosis and several antibacterial agents [30]. Biofilm formation is accounted for as a major problem in biomedical applications, which is one of the reasons for biomaterial-associated infections [33]. Thus, inhibiting biofilm formation and lowering bacterial adherence are more effective antibacterial techniques than killing germs [30], [34].

- **Capsules**

Another bacterial defense mechanism is the bacterial carbohydrate capsules [30] [31], which, throughout acute inflammatory and adaptive immune responses, bacterial capsules shield bacteria from phagocytosis [30]. Bacteria release capsules that cling to their cell walls, and they help mucosa and skin adhere and

store nutrients and water [30]. Capsules occur in gram-negative bacteria such as *E. coli* [30].

2.2 Antibacterial Biomaterials

The development of new antibacterial bio-materials is urgently needed to enhance bacterial selectivity, decrease antibiotic resistance, and overcome the other issues of traditional antibacterial agents, so several antibacterial biomaterials were developed [29]. These materials can be categorized into many different categories, including:

- inorganic-based antibacterial biomaterials such as metallic NPs.
- polymeric biomaterials, including antimicrobial peptides (AMPs), quaternary ammonium salt derivatives, host-defense peptides (HDPs), etc.
- antibacterial biomaterials conjugated with antibiotic derivatives [29].

2.2.1 Antibacterial polymers (APs)

The interest in macromolecular antibacterial agents and their nanostructured applications has been growing because they play an important role in overcoming issues with antibacterial therapeutic agents. These macromolecular compounds can be inherently antibacterial polymers or polymer-conjugated antibacterial agents [35] [36].

Antibacterial polymers (APs) are a potentially promising class of antibacterial therapeutic agents with distinctive properties for combating BIs diseases. They draw great research interest in academia and industry due to their low toxicity, long half-life, chemical stability, non-volatility, and superior efficacy compared to other molecules [35] [36].

Moreover, due to their different mechanisms against bacteria, APs are classified into two different types: passive and active APs. Passive APs restrict bacterial growth by reducing bacterial adherence to surfaces. Active APs, on the other hand, either interact with the bacterial cell wall and damage their cytoplasmic membranes or interfere with the fundamental intracellular functions of bacteria [37]. The antibacterial activity of these polymers is based on different parameters, including their size, morphology, and surface charge [38].

- Inherently Antibacterial Cationic Polymers (IACPs)

Polymers having positive charges or formed with cationic groups on their backbone and/or side chains are called cationic polymers. They have recently been the subject of intense research as promising candidates for antibacterial systems [38]. They are attractive for use in a wide variety of biological applications because of their distinct physicochemical features and their ability to undergo modifications, such as drug delivery systems, tissue engineering, water treatment systems, bioimaging, biosensor systems, and antibacterial applications. Typically, they are categorized as either natural polymers such as chitosan, gelatin, dextran, and cellulose, or synthetic polymers like polyethylenimine (PEI), poly(amidoamine)s (PAMAMs), poly(amino-co-ester)s, and quaternary ammonium polymers. In addition, hybrid copolymers of natural and synthetic polymers are also in use as antibacterial polymeric structures [39]. Thanks to the presence of reactive sites in most of these polymers, they can be modified to improve their physicochemical features in order to make them more effective as inherently antibacterial systems to minimize, prevent, or control bacterial infections [38].

The APs with quaternary ammonium groups have inherent positive charges independent of pH, unlike the primary, secondary, and tertiary ammonium groups, which can only be developed by protonating their amines and have relatively strong antibacterial efficacy and little hemolytic activity. These polymers are called inherently antibacterial cationic polymers (IACPs) [40] [41]. Although cationic polymers provide an affordable alternative, their significant charge-associated toxicity makes them undesirable. Therefore, it is necessary to balance the amphiphilicity of these polymers to address this issue and make them more biocompatible. This change not only makes these polymers less harmful to cells but also makes them better at breaking down membranes. By cooperatively interacting with the bacterial cell membrane, the amphiphilic polymers break up the transmembrane potential, which lets cytoplasmic material leak out of the cell and kills it [42].

IACPs have received the greatest attention in research since, unlike antibiotics, they are less likely to produce significant bacterial drug resistance [43]. Furthermore, they have distinctive features including antibacterial capabilities without the requirement for any antibacterial agent, biocompatibility, and ease of production and modification [43] [40]. As a result of this direction, much effort has been made to encourage their progress.

The two primary functional components of IACPs are cationic and hydrophobic groups. Their antibacterial activity relies heavily on both of these two groups. As a result, these groups must be carefully chosen in order to achieve the desired level of antibacterial activity [40]. Sulfonium ions, ammonium ions, phosphonium ions, and many other ions are all viable possibilities for cationic centers [40]. The antibacterial activity of APs is often impacted by the length of their hydrophobic groups, which are typically hydrophobic alkyl chains that have the ability to penetrate the bacterial membrane [40].

According to the research of Engler et al., the minimum inhibition concentrations (MIC)s of cationic polymethacrylate derivatives for different types of pathogenic bacteria drop with the increase of chain spacer length between 3 and 8 carbons [44]. This is because the longer chain provides more hydrophobicity to the polymer, resulting in better interaction with the lipid bilayer of bacterial membranes and hence enhancing the antibacterial effectiveness. It's important to note that the chain length must be within a certain range because excessive lengthening results in aggregate polymers, thus decreasing antibacterial activity [45] [46]. Therefore, it is important to find the optimum chain length for these groups.

This thesis focuses on NPs made from a polymer with ammonium-based cationic groups because they can be used in a wide range of biomedical application areas [40].

Electrostatic interactions between polymer positive charges and bacterial cell membrane negative charges make them show special selectivity for bacteria. The negative charge from gram(+) bacteria's teichoic acid and gram(-) bacteria's phospholipids allows the polymer's cationic group to adhere to the surface of the

bacteria's membranes. Then, the polymer's hydrophobic group penetrates and disrupts the bacterial membrane, killing pathogenic germs. Thus, cationic and hydrophobic groups immediately damage the bacterial cell membranes and give the polymer antibacterial activity [43] [40].

- **Quaternized poly(4-vinylpyridine) (P4VP)**

Poly(4-vinylpyridine) (P4VP) is a basic polymer that bears pyridine rings [47]. The tertiary nitrogen in the pyridine ring makes this polymer pH sensitive [47]. P4VP is insoluble in water, while it becomes water-soluble when the tertiary amine group is protonated below pH=5 ($pK_\alpha \sim 5$) [48]. In addition, tertiary amine groups of P4VP can be alkylated to produce a quaternary ammonium ion, which has permanent positive charges (Figure 2.4) [49]. By using different alkylating agents, the hydrophobicity-hydrophilicity, and functional groups of the polymer can be easily modified [11]. This endows them with distinctive properties, including strong binding interactions with molecules and surfaces that have opposite charges, such as cell membranes, and high water solubility [47]. As a result, they are effective and suitable materials for a variety of applications such as water treatment [50], tissue engineering [51], cosmetics [47], and sensors[52], as well as biomedical applications[47].

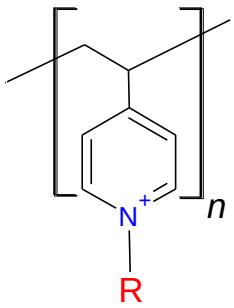


Figure 2.4 Quaternized P4VP chemical structure

Positively charged quaternary ammonium P4VP is a good example of inherently antibacterial cationic polymers [43]. Contrary to other antibacterial cationic polymers, such as CS [38] and PEI [20], it includes nitrogen covalently bound to four groups and is positively charged regardless of pH [40] [43]. It inhibits the growth of both gram-positive and gram-negative bacteria [40]. Also, hydrophilic parts like oligoethylene glycol groups (OEG, OEGMA) can be added to these

polymers to help keep the amphiphilic balance and reduce cytotoxicity, resulting in the formation of quaternized amphiplic copolymer [43] [40].

Figure 2.5 represents the antibacterial mechanism action of quaternized amphiphilic copolymer [53]. Polycation chains adher electrostatically to the negatively charged cell membrane surface, followed by the insertion of hydrophobic groups into the cell membrane of bacteria resulted in formation of amphiphilic conformation thus disrupt bacterial membrane and bacterial death [53].

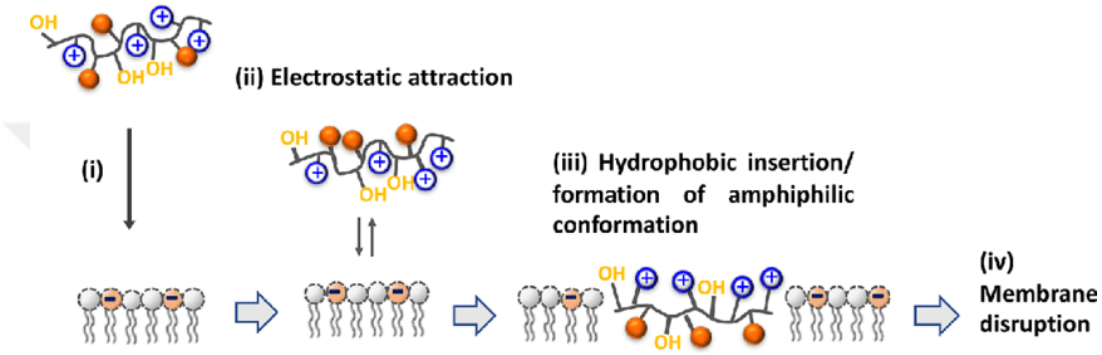


Figure 2.5 Antibacterial mechanism action of amphiphilic polycations [53]

2.2.2 Antibacterial Nanoparticles

Nanotechnology provides novel physiochemically modified nano-materials with superior antibacterial features to be more effective than their bulk materials and improved in addressing multi-drug resistance [9], biofilm formation [54], and other traditional antibacterial agents issues [9] . Consequently, various classes of NP-based antibacterial materials have attracted great interest among the other traditional antibacterial agents due to their direct contact with the bacterial cell wall without penetrating the cell, which makes them less likely to be exposed to most antibiotic resistance mechanisms [32]. This increases the likelihood of NPs being used to treat or prevent bacterial infections [32].

NP-based antibacterial materials are now regarded as viable alternatives to antibiotics due to their efficacy in treating BIs [55]. Due to the NPs' multiple mechanisms that are all active at the same time, bacteria cannot evolve simultaneously multiple gene mutations, hence they are less likely to develop multiple resistance [32].

They can be either inherently antibacterial NPs or antibiotic-loaded NPs [55]. Several inherently antibacterial NPs have been reported to be used directly as antibacterial agents, such as inorganic NPs [56] or organic NPs [57] (e.g. silver (Ag) NPs [58], and chitosan NPs [54] respectively), or as effective nanocarriers to deliver antibacterial agents in a controlled manner at their infected area with the decreasing of drug leakage outside the targeted-site and the reducing the side effects including polymeric NPs [56], lipidic nanocarriers [56], chitosan-based nano-biopolymer [59], metallic nanocarriers [54], silver-liposome [60], polymeric micelles [54], dendrimers, carbon nanotubes [61], graphene [56], aqueous fullerene NPs [62] [56].

NPs can be used in different antibacterial applications, such as antibiotic delivery systems, antibacterial coating for medical devices, bacterial detection, wound dressing, etc [32].

Bacterial tolerance or resistance to NPs can be affected by different factors, such as

- Bacterial cell wall membrane structures, which are different between the Gram (-) and Gram (+) bacteria as mentioned before [63],
- Bacterial growth rate, NPs are more effective against fast-growing bacteria [64],
- NPs and biofilms interact based on their electrostatic features [55].

➢ **Antibiotic-Loaded Nanoparticles**

NPs can be used effectively as antibacterial agent carriers [32]. This combination of two different materials seems to be a highly appealing approach for treating BIs [9]. In general, antibiotic molecules are small organic molecules compared to polymers. If the average size of the antibiotic is larger, it reduces its ability to penetrate the bacterial cell membrane and needs to be delivered to intracellular bacteria [32][65]. The NPs can easily enter the host cells by endocytosis and release the antibiotic intracellularly due to their small size and flexible structure [32] [66]. So, the ultra-small, and controllable size of NPs is the main feature that makes them superior delivery systems of antibiotics compared to conventional carrier systems [67]. This characteristic enhances their ability to combat

intracellular germs and conduct antibacterial activities [67]. Furthermore, NPs provide both antibiotic protection against undesired chemical reactions and target antibiotics to the BIs site, hence preserving their potency and reducing antibiotic systemic side effects [32]. Using antibiotic-loaded NPs, compared with free antibacterial agents, the optimum antibiotic-effective concentration level is maintained at the targeted site for a prolonged time thus decreasing the dosage frequency, and improving stability [32].

- **Inherently Antibacterial NPs**

As mentioned before, another type of NPs used in antibacterial applications can be made up of inherently bactericidal materials such as metallic, polymeric, and ceramic materials [2]. These antibacterial materials are used in various bio-applications [2]. These types of NPs, compared to their bulk materials, show better antibacterial activity, due to their superior properties including their high surface area, dissolution rate, catalytic activity, etc [4]. Good examples of that are Fe_3O_4 nanoparticles, which are antibacterial in NP form but not in bulk [9], and quaternized PEI NPs [20].

- **Inherently Antibacterial Metallic NPs**

The antibacterial activities of metallic NPs, such as copper [68], silver [69], and gold NPs [70], have been reported in many publications [71].

Although the antibacterial mechanism of metallic NPs is still poorly understood, it does seem to be based on particle-specificity [9]. So, to explain and understand their bactericidal mechanism according to the change of structure and morphology in bacterial cells, several hypotheses have been proposed (Figure.2.6) [9].

I. Nanoparticles can adhere to and penetrate bacterial cell walls, producing structural alterations in cell membrane permeability and cell death [72]. Silver NPs, for example, have a higher surface area than other metallic NPs and so attach better to the bacterial cell membrane, leading to more efficient antibacterial activity [73].
II. Nanoparticles generate free radicals that may damage cell membranes and lead to cell death [74]. Metallic NPs in bacterial cells may interact with soft bases (such as sulfur and phosphorus), damaging the DNA and killing the cell [74].

III. NPs may affect how bacteria send and receive signals by dephosphorylating peptide substrates on tyrosine residues. This inhibits bacterial growth, hence cell death [75].

IV. Metallic NPs can release ions that can bind with the thiol groups of many cellular enzymes and make them inactive, thereby disrupting their cellular activity [76] [77].

V. NPs inhibit bacterial growth either by decreasing the ribosomal subunit link to tRNA or by decreasing the ATP level by inhibiting the ATPase and collapsing the membrane potential [78].

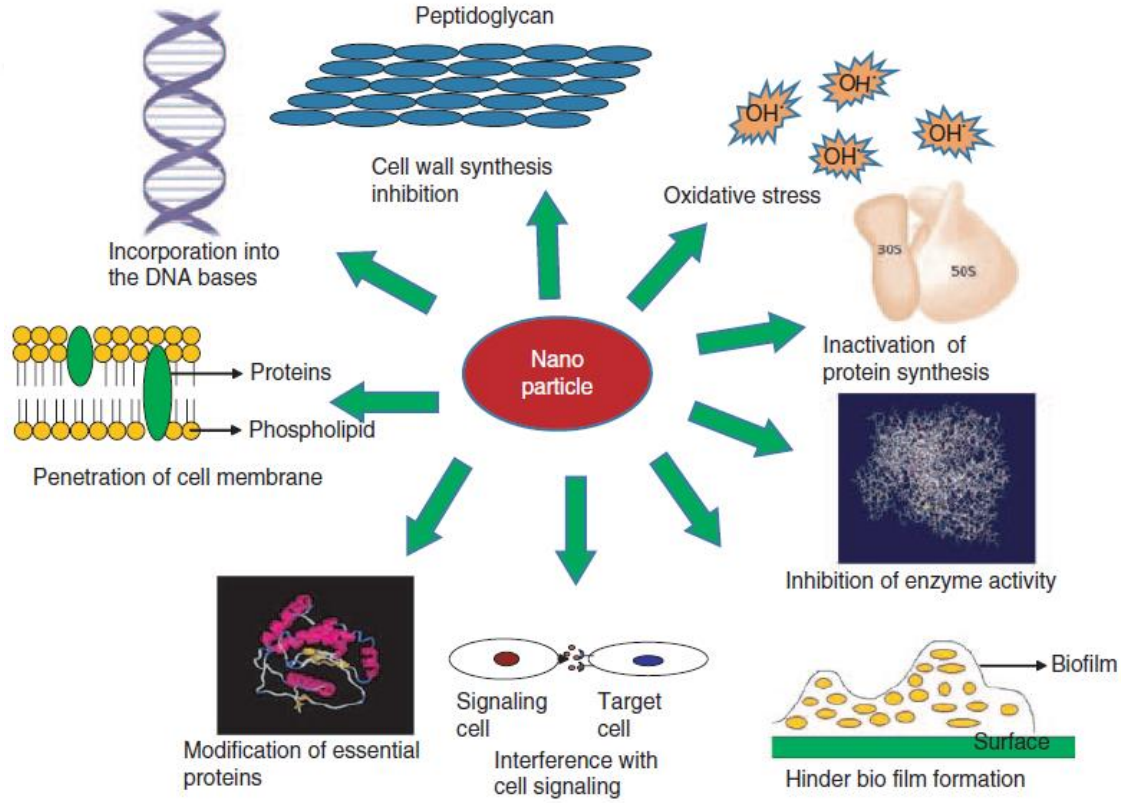


Figure 2.6 The antibacterial mechanism of metallic NPs [9]

- **Copper nanoparticles (CuNPs)**

Copper serves as a cofactor for a number of vital enzymes, including cytochrome C oxidase and ceruplasmin [79]. Cu has different roles depending on its oxidation state. The reduced Cu^{+} has a strong affinity for thiols and thioethers [80]. The oxidized Cu2+ favors oxygen or nitrogen groups [79]. Copper interacts with proteins and hence plays an important role in many biological processes [79] [80].

The specific mechanism of Cu ions' antibacterial action, is well unknown, however, bacterial cell death is predicted to be caused by a number of distinct mechanisms, including rupture of the cell membrane, intracellular change of metabolic processes, and production of DNA damage [81] [82]. So, copper nanoparticles (CuNPs) can damage bacterial structures, disrupting metabolic activities through the interaction of Cu2+ ions with phosphorus and sulfur in DNA and proteins [68]. As a result of their antibacterial activity, they have been used in a variety of biomedical applications to enhance and provide bactericidal properties to the designed material [68] [83].

The antibacterial properties of CuNPs against *E.coli* cells were reported by Chatterjee et al. [84]. They demonstrated that CuNPs cause several toxic effects in *E. coli* cells, including ROS production, protein oxidation, lipid peroxidation, and DNA fragmentation resulting in *E.coli* cells death. They demonstrated that Cu2+ ions play a crucial role in DNA fragmentation and these ions are also responsible for the increased reactivity of CuNPs compared to that of their precursor, CuCl2 [84].

- **Silver nanoparticles (AgNPs)**

Silver ions (Ag+) are poisonous to bacteria, viruses, fungi, and other species [85][86], but not to humans [87]. Due to their features, silver-based nanoparticles (AgNPs) are gaining popularity in various bioapplications. Size, shape, and surface may be adjusted during synthesis, and biochemical functioning can be tuned [88]. Silver is reported in the literature as an antibacterial with a wide range of applications, and its antibacterial activity was reported for the first time in the 1800s [69]. Thus, AgNPs have been intensively studied as a nanomaterial for killing bacteria [89]. AgNPs have antibacterial activity and ionic silver characteristics due to the spontaneous release of Ag+ from their surface [89].

AgNPs have many antibacterial properties, making them superior antibacterial materials [2]. These NPs are effective against both gram-positive and gram-negative bacteria. Moreover, they are less likely to develop bacterial resistance, particularly in gram-negative bacteria [90]. The good antibacterial features of

silver nano-crystallites, which were biosynthesized, against Gram-negative and Gram-positive bacteria were reported by Suresh et al. [91].

Different potential antibacterial mechanisms of AgNPs are reported:

- The positive Ag+ ions, which are released from AgNPs, interact with the negative bacterial cell membrane, resulting in cell wall membrane structure alterations and an increase in cell permeability, which ultimately results in cell death [92].
- External and internal components containing phosphorous and sulfur are more likely to interact with AgNPs, and these interactions affect cell division, oxygen uptake, and ultimately cell survival [69].
- Ag+ has a strong affinity for nitrogen and sulfur, may disrupt protein structures by forming bonds with thiol and amino groups [93]. It has been hypothesized that reactive oxygen species (ROS) are produced when NPs are bound to thiol groups; these ROS inhibit respiratory enzymes and may be deadly [69].
- Ag+ ions show antibacterial activities because they can interfere with bacterial DNA replication by binding to sulfhydryl groups in proteins and interacting with the peptidoglycan of the bacterial cell wall membrane and the plasma membrane [92].

Long et al. [94] studied the morphology of *E. coli* cells following AgNPs treatment with 1 mM GSH. The bacteria given more GSH were smooth and undamaged and closely resembled the non-treated control samples, demonstrating that AgNPs-treated cells collapsed due to oxidative stress [94].

- **Some drawbacks of metallic NPs**

Although metallic NPs have excellent inherent antibacterial efficacy, they have drawbacks that prevent them from being widely used [95]. Metallic NPs could accumulate over time in the different organs of organisms like the kidneys, liver, lungs, and spleen, causing metallic NPs to enter biological systems, which can cause undesired issues for the organism [95]. Furthermore, they are time- and dose-dependently toxic and may destroy some organelles, such as mitochondrial DNA [96]. This limits the use of metallic NPs against some bacteria, such as *Helicobacter Pylori* [96]. Their toxicity is affected by several parameters like dose,

size, structure, other physicochemical features, surface properties, and exposure pathways [95]. Even when certain metallic NPs were toxic, altering their surface charge or coating might reduce or remove their toxicity [95]. Studies focused on the toxicity of metallic NPs are still poor, and toxicological research on metallic NPs' optimal dosage, frequency of exposure, duration, and potential effects and actions is still needed.

❖ **Inherently antibacterial Polymeric NPs**

Recently, the majority of studies have been interested in the development of innovative and novel strategies to overcome the drawbacks of conventional antibacterial agents [97].

Due to the vital role of the negatively charged bacterial cell membrane for bacterial survival, it is a prime target for antibacterial agents [98]. It makes sense to produce antibacterial compounds with cationic charges [99]. Therefore, antibacterial polymeric nanosystems that mimic the cationic and amphiphilic characteristics of naturally occurring antibacterial peptides [100] have been developed [101].

As mentioned before, cationic polymers including synthetic [102] (i.e., conjugated [103], block [104], and random [105] copolymers) and natural polymers [38], incorporated with hydrophobic moieties are utilized in antibacterial biomaterials [43]. They mimic the antibacterial mechanisms of AMPs, which produce antibacterial activity by disrupting cell wall membranes, thus decreasing bacterial resistance [101]. AMPs are cytotoxic because they lack target specificity, and by emulating their structure, most antibacterial polymers also have varying cytotoxic effects on mammalian cells [101]. Therefore, using these polymers to produce antibacterial cationic polymeric NPs and controlling their charge density can improve antibacterial activity and biocompatibility [97][101]. Highly positively charged molecules have good antibacterial activity but low biocompatibility [101]. Whereas neutral hydrophilic moieties added into these systems to reduce charge density can increase biocompatibility while having no effect on the antibacterial effectiveness [101].

In this study, the surface of PLGA NP has been coated with different amounts of a quaternized poly(4VP-co-OEGMA) copolymer to produce differently-sized cationic polymeric NPs with inherent antibacterial properties, and the produced inherently antibacterial NPs do not release any drug. These NPs have the potential to be used in different biomedical applications such as drug delivery systems, surface coatings, and wound dressings.

3
MATERIALS AND METHOD

3.1 Materials

Table 3.1 Materials used in the thesis study

Chemical Name	Company	Purpose of usage
4-Vinylpyridine	Sigma-Aldrich	Polymer synthesis
Poly(ethylene glycol) methyl ether methacrylate, Mw 500 Da	Sigma-Aldrich	Polymer synthesis
4-4'-Azobis(4-cyanovaleric acid)	Sigma-Aldrich	Initiator
1-Bromohexane	Sigma-Aldrich	Quaternization agent
1,6-Dibromohexane	TCI	Crosslinker
N,N-Dimethylformamide	ISOLAB	Solvent
Diethyl ether	Sigma-Aldrich	Solvent
Ethanol	Sigma-Aldrich	Solvent
Poly(D,L-lactide-co-glycolide), Mw7-17 kDa	Sigma-Aldrich	PLGA NPs synthesis
Acetone	ISOLAB	Solvent
2-Propanol	ISOLAB	Solvent
Fibroblast cell culture (L929)	YTU- Cell Culture and Tissue Engineering Laboratory	Biocompatibility Test - Cell culture
FBS (Fetal Bovine Serum)	Capricorn	Biocompatibility Test

Table 3.1 Materials used in the thesis study (continued)

Dulbecco's Modified Eagle Medium (DMEM/F12)	Capricorn	Biocompatibility Test - Cell culture
Penicillin-streptomycin	Capricorn	Biocompatibility Test
Dimethyl sulfoxide	Sigma Aldrich	Biocompatibility Test
Trypsin-EDTA (0.25%)	Sigma Aldrich	Biocompatibility Test - Cell culture
MTT [3-(4,5-dimethylthiazol-2yl)-2,5-diphenyltetrazolium bromide]	Biomatik	Biocompatibility Test
Both Muller Hilton Agar	Sigma Aldrich	Antibacterial activity assay
Muller Hilton broth	Sigma Aldrich	Antibacterial activity assay

1.4 Equipment

Table 3.2 Names and brands of devices used in the thesis study

Device Name	Brand/Model
Scanning Electron Microscope	FEI (PHILIPS) XL30 SFEG SEM
NMR	Bruker Avance 500
FT-IR Spectrometer	Nicolet™ iS™ 10
GPC	Viscotek TDA302
Dynamic and Electrophoretic Light Scattering Spectroscopy	Malvern Zetasizer NanoZS and Ultra
Lyophilizator	Telstar Cryodos

Table 3.2 Names and brands of devices used in the thesis study (continued)

Vortex	Heidolph Reaxtop
Analytical Balance	Precisa
Refrigerated Centrifuge	Sigma
Vacuum Oven	Binder
Ultra-Pure Water Device	Millipore MilliQ Gradient
Magnetic Stirrer	Heidolph
Laminar flow cabin	Faster and ESCO class II
Incubator	Binder and Memmert UN55
Invert microscope	Olympus
Centrifuge	Himac
Microplate reader	Multiskan™ FC
Multiwell plate reader	Biotek Powerwave XS2
Refrigerated oven	JSR

3.2 Experimental Methods

This study aimed to produce inherently antibacterial cationic nanoparticles and examine the effect of their size on their antibacterial activity against gram-positive and gram-negative bacteria.

The major steps to be followed for this purpose are grouped under the following three headings, respectively:

1. Synthesis and characterization of cationic poly(4VP-co-OEGMA) copolymers
2. Synthesis and characterization of 4VP-based cationic nanoparticles in different sizes
3. Investigation of the antibacterial effect and biocompatibility of produced materials.

The experimental method to be carried out in the study is shown schematically in Figure 3.1.

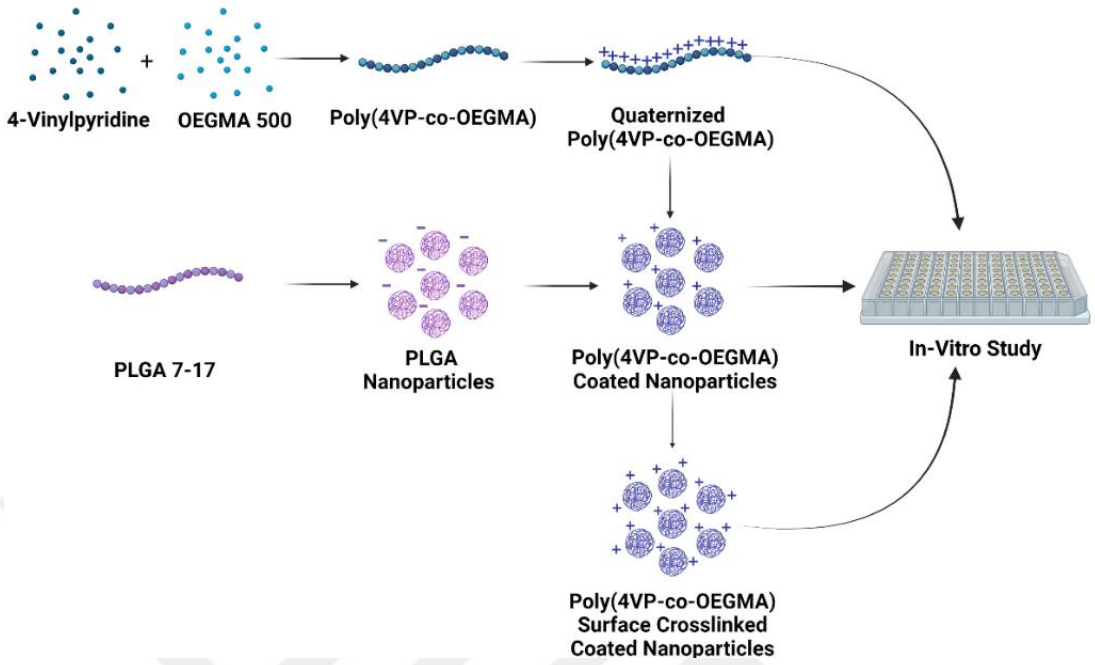


Figure 3.1 Schematic representation of the experimental method

3.2.1 Synthesis of Cationic Poly(4VP-co-OEGMA) Copolymer

Poly(4VP-co-OEGMA) random copolymer required for obtaining a cationic polymer with antibacterial properties was synthesized by free radical polymerization of 4-vinylpyridine (4VP) and poly(ethylene glycol) methyl ether methacrylate OEGMA (Mw = 500 Da, OEGMA500) monomers (Figure 3.2). 4-4'azobiscyanoleric acid (ACVA) was used as the initiator, and dimethylformamide (DMF) was used as a solvent [106].

0.9 M of 4VP and 0.1 M of OEGMA500 monomers were dissolved in DMF. The solution was purged with N_2 gas for 20min to eliminate the dissolved oxygen, and the solution was heated to 70°C. Then, the polymerization was started by adding ACVA solution to the monomer solution. The initial molar ratio of the monomer to the initiator ($[M]_0/[I]_0$) was 100:2. The free radical polymerization was carried out for 24h.

The copolymer obtained after 24h was precipitated with excess cold diethyl ether. The polymer was dissolved in methanol and precipitated in excess cold diethyl

ether again to remove the unreacted monomers and DMF. The final product was vacuum-dried for 24h at 50 °C. The obtained copolymer was chemically analyzed by FT-IR and ^{1}H-NMR spectroscopy, and its Mw was determined by GPC.

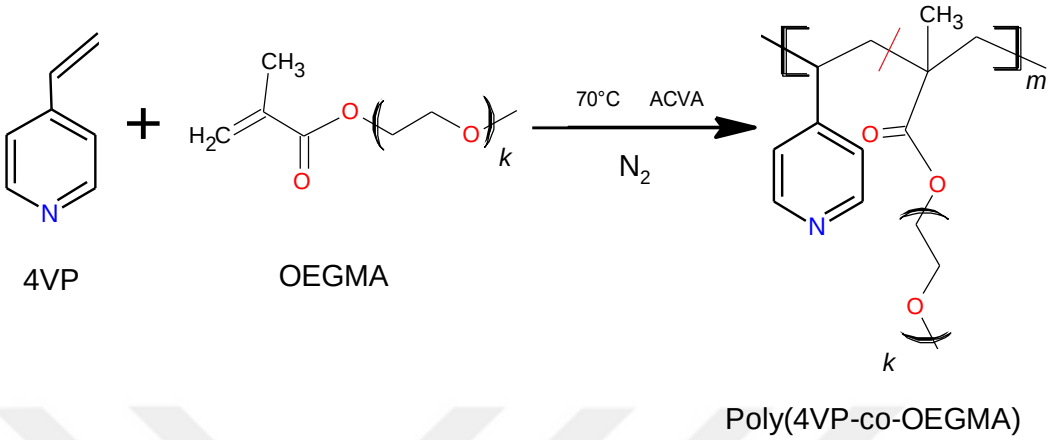


Figure 3.2 Free radical polymerization of poly(4VP-co-OEGMA) copolymer

To obtain a cationic copolymer, the produced copolymer was quaternized with 1-bromohexane (BrH) (Figure 3.3). For this purpose, BrH was added to provide 40% quaternization [43] by dissolving the polymer in 2-propanol, and the quaternization reaction was carried out at 70 °C for 3 days. After the reaction was completed, the obtained polymer was precipitated with excess cold diethyl ether and dried. To eliminate the residual BrH and 2-propanol, the precipitate was dissolved in methanol and precipitated twice, and then it was dried in a vacuum oven at 50 °C for 24 h. The obtained polycation was chemically analyzed by FT-IR, DLS, and ELS.

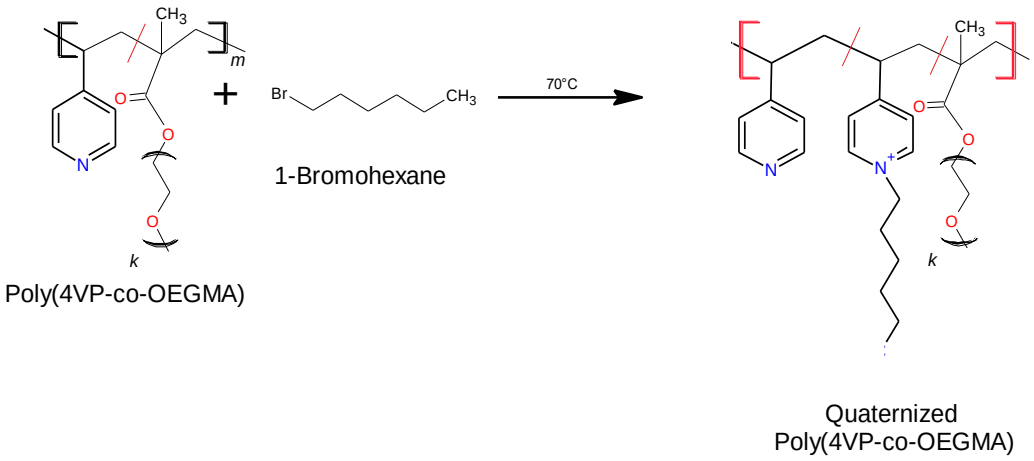


Figure 3.3 Quaternization reaction of poly(4VP-co-OEGMA) copolymer

3.2.2 Synthesis of Polycationic Coated NPs

To produce different sizes of NPs, PLGA NP were coated with different concentrations of quaternized poly(4VP-co-OEGMA) copolymer. In the first step, 0.5 mg/mL PLGA NP solution was prepared by nanoprecipitation. For this purpose, PLGA (5 mg) was dissolved in 0.5 mL acetone, then it was added drop by drop to 10 mL ultra-high pure water. The solution was stirred vigorously for 5h to ensure evaporation of the acetone.

In the second step, the produced PLGA NP was mixed with different concentrations of quaternized poly(4VP-co-OEGMA) copolymer. For this purpose, 8 different solutions were prepared. In all solutions, the concentration of PLGA NP was kept constant at 0.5 mg/mL. Eight different concentrations of quaternized poly(4VP-co-OEGMA) were prepared separately in 0.5 mL of ultra-pure water. Then, the polycation solutions were added onto PLGA NP solutions. The final concentrations of the polycation were 0.67, 2.00, 3.33, 6.67, 13.33, 33.33, 53.33, and 66.67 mg/mL (Table 3.3). The solutions were stirred for at least 15 minutes.

To crosslink the surface of the obtained polycationic-coated NPs, 1.2 uL of 1,6-dibromohexane (DBH) was added to all the obtained coated NP solutions, and the reaction was carried out at 70 °C for 24h.

Table 3.3 Codes and concentrations of non-crosslinked NPs (NC-NPs) and surface crosslinked polycationic NPs (SC-NPs)

NC-NPs	C_{PLGA} mg/mL	$C_{Polyctions}$ mg/mL	SC-NPs	C_{PLGA} mg/mL	$C_{Polyctions}$ mg/mL	C_{DBH} uL
NC1	0.5	0.67	C1	0.5	0.67	1.2
NC2	0.5	2.00	C2	0.5	2.00	1.2
NC3	0.5	3.33	C3	0.5	3.33	1.2
NC4	0.5	6.67	C4	0.5	6.67	1.2
NC5	0.5	13.33	C5	0.5	13.33	1.2
NC6	0.5	33.33	C6	0.5	33.33	1.2
NC7	0.5	53.33	C7	0.5	53.33	1.2
NC8	0.5	66.67	C8	0.5	66.67	1.2

3.2.3 Characterization

- **Fourier Transform Infrared Spectroscopy (FT-IR) analysis**

The molecular structures, and quaternization degrees of poly(4VP-co-OEGMA) copolymer Equation 3.1 [107] and all synthesized NPs were detected using Fourier Transform Infrared Spectroscopy (FT-IR), which depends on the absorption of light in the infrared range of the electromagnetic spectrum and forms absorption bands at different wavelengths specific to the bonds in the molecular structure.

The copolymer and dried NPs were placed on the reduced total reflectance (ATR) apparatus of the Shimadzu IRPrestige-21 FIR spectroscopy, and the FT-IR spectrum was acquired within the range of 4000-650 cm^{-1}.

$$QD\% = \frac{A_{1640}}{A_{1640} + (1.68 * A_{1600})} * 100 \quad (3.1)$$

- **NMR Spectroscopy**

To determine the molecular structure of the poly(4VP-co-OEGMA) copolymer and the monomer quantities in its chain, NMR spectroscopy was used. The ^{1}H-NMR spectrum of the polymer was obtained using Bruker Avance 500 NMR spectroscopy. The spectrum was taken by dissolving the polymer sample in deuterated DMSO.

- **GPC Analysis**

The molecular weight and molecular weight distribution of the synthesized poly(4VP-co-OEGMA) copolymer were determined using the Viscotek TDA302 GPC system with a refractive index and light scattering detectors. Separation was performed with an Eprogen CatSEC300 column, and the flow rate was set at 0.30 or 0.25 mL/min. A 0.1 M acetic acid solution containing 0.15 M NaCl was used as the mobile phase. The samples were filtered with a 0.45 μm syringe filter before the analysis.

For adsorption studies, NPs were centrifuged, and the supernatants were analyzed with GPC to determine the concentrations of free quaternized poly(4VP-co-OEGMA) copolymers by comparing to the chromatogram of a standard polymer. The samples were filtered with a 0.45 μm syringe filter before the analyzes.

- **Dynamic and Electrophoretic Light Scattering Spectroscopy**

Malvern Zetasizer Nano ZS device was operated at 25 ℃ for hydrodynamic size, hydrodynamic size distribution, and zeta potential analysis of the obtained NPs. Single convoluted capillary cuvettes were used for both dimensional and zeta potential analyses.

Malvern Zetasizer Ultra device was used for counting NPs numbers. Only NC-NP samples were analyzed. Each sample was diluted with ultra-high pure water to obtain a final polycation concentration of 1 mg/mL.

- **Scanning Electron Microscopy**

The morphological properties of NPs were determined and provided as high-resolution images by Electron Microscope FEI (PHILIPS) XL30 SFEG (SEM). For this purpose, the dried PLGA, NC1, NC3, and NC7 NPs were sputter coated with gold-palladium under Argon gas for 1h. The area was then imaged with an emission gun of SEM. High-resolution images were obtained at different magnifications.

3.3 In-Vitro Tests

3.3.1 Antibacterial Activity Test

Antibacterial activity of quaternized poly(4VP-co-OEGMA), NC-NPs, and SC-NPs obtained in this study was evaluated by the broth microdilution method on *Staphylococcus aureus* (ATCC 25923) and *Escherichia coli* (ATCC 25922).

- **Preparation of Medium**

Commercial Muller Hilton Agar (MHA) and Muller Hilton Broth (MHB) media were dissolved in distilled water at a concentration of 34.0 g/L and autoclaved. The obtained medium was sterilized in an autoclave at 125℃ for 15min, poured into sterile Petri dishes as 12.5 mL each, and kept at room temperature until solidified.

PBS (Phosphate buffer solution) was prepared to provide the pH conditions in the living bacteria in antibacterial tests. For the preparation of PBS solution, the total

volume is 500 mL, 8 g/L sodium chloride (NaCl), 0.2 g/L potassium chloride (KCl), 1.44 g/L disodium phosphate (Na_2HPO_4), 0.24 g/L monopotassium phosphate (KH_2PO_4) was dissolved in distilled water. The resulting solution was then stored at +4 ℃ to be used in the experiments.

- **Preparation of Bacterial Suspensions**

E.coli and *S.aureus*, selected reference microorganisms in this study, were inoculated into MHB medium by taking a single colony. It was incubated in a shaking incubator for approximately 18h at 200 rpm at 37 ℃. The next day, bacterial cultures were diluted with MHB medium until the absorption of the culture reached 0.1-0.2 at 600 nm (1.5-3.0 $\times$ 10^8 CFU/mL concentration).

- **Broth Microdilution Method**

Quaternized poly (4VP-co-OEGMA) copolymer, NC-NPs, and SC-NPs obtained in this study were prepared in a wide range of concentrations, and they were analysed by the broth microdilution method based on CLSI principles [108]. The Minimum Inhibitory Concentration (MIC) values of the produced polymeric NPs were determined using this method. 1 mg of each sample was dissolved in 1 mL of distilled water (stock solutions). For MIC analysis, a 96-well plate was used to make step-wise dilutions of stock solutions in MHB (6.25,12.5, 25, 50, and 100 μg/mL). Then, 100 μl of *E. coli,* and *S. aureus* (10^6 CFU mL-1) were taken separately and added to the test samples. The 96-well plates were incubated at 37℃ overnight (18h). On the other hand, the negative control was only broth and bacteria without any sample solution, and the blank control was the broth that was not inoculated with bacteria. At the end of the incubation, the MIC value was determined by measuring the microbial growth in the wells spectrophotometrically, Optical Density measurement, (OD600 nm) and MIC values were confirmed by the standard plate counts method. The study was carried out in triplicate.

In addition to MIC values, MOI (multiplicity of infection) values were also determined to correlate the antibacterial activity not only with the polymer

concentration but also with the particle number. For this purpose, the equation of MOI [109] has been modified as Equation 3.2.

$$\text{MOI} = \frac{\text{The number of NPs (Infectious agents)}}{\text{The number of bacteria (Infection Targeted)}} \tag{3.2}$$

3.3.2 Biocompatability Test – MTT

- **Cell culture**

L929 fibroblast cells were used in cell culture studies. These cells were grown in Dulbecco's Modified Eagle Medium (DMEM/F12) growth medium containing 10% FBS and 1% penicillin-streptomycin in an incubator set to 5% CO2, 95% humidity, and 37 ℃. When cells reached 70–80% confluency in 75T culture dishes, they were passaged with 0.25% trypsin-EDTA solution [110]. Cells collected during this procedure were centrifuged at 1000 rpm and 25ºC for 5 min, and then the supernatant was discarded, and the remaining cell pellet was suspended with 1 mL of growth medium. Cells were counted on the Thoma slide with trypan blue, and the required number of cells were taken into the growth medium.

- **MTT method**

The cytotoxicity of the previously obtained NC-NPs and SC-NPs (group-1, and group-2, recpectively) at different concentrations (4, 8, 16, 32, 64 and 128 μg/mL) was determined by MTT [3-(4,5-dimethylthiazol-2yl)- 2,5-diphenyltetrazolium bromide] method.

The yellow-colored tetrazolium dissolved in water as the MTT salt used in this method is converted into a water-insoluble, purple-colored formazan by mitochondrial activity in the cell [111]. Thus, by quantifying formazan, information about the current cell viability is obtained.

For the MTT test, cells were seeded into 96-well plates at 105 cells/mL in each well and the plates were kept under incubation conditions for 24h. At the end of this period, all NPs were applied to the cells. Before they were added on the cells, the polymeric nanoparticles were sterilized with UV light for 45min/ All dilutions of nanoparticle solution were accomplished with the growth medium. After applying different concentrations of NPs to the cells, the plates were incubated for

72h. Then, 10 μL of the 10 mg/mL MTT solution prepared with 1X PBS was added to each well and incubated in the dark for 4h. After this period, 100 μL of dimethyl sulfoxide (DMSO) was added to each well to dissolve the formazan crystals formed, and the plates were kept in the dark for 30min. In a microplate reader (Multiskan™ FC), the optical density of the plates was measured at 570 nm. Cell viability (%) was calculated by using the obtained absorbance data in Equation 3.3 [112]. The cell viability of the control group was evaluated at 100%, and the data of each group were compared with the control group and plotted. Each sample was evaluated in triplicate, and ±SD was calculated. At the same time, IC_{50} values on fibroblast cells were calculated using the concentration-cell viability (%) plot for each group.

$$\text{Cell viability (\%)} = (OD_{sample}) / (OD_{control}) \times 100\% \quad (3.3)$$

4
RESULTS AND DISCUSSION

In this thesis, PLGA NPs were coated by a quaternized poly(4VP-co-OEGMA) copolymer to produce differently sized inherently antibacterial NPs. In addition, surface groups of coated NPs were crosslinked to stabilize the structure and investigate the crosslinking effect. Then, the biological activity and performance of NPs depending on their size were evaluated by antibacterial activity assays against both gram-positive and gram-negative bacteria, and biocompatibility tests on mammalian cells. In this context, the study has been accomplished by following the steps below:

- Synthesis of antibacterial quaternized poly(4VP-co-OEGMA) copolymer,
- Production of differently sized NPs coated with quaternized poly(4VP-co-OEGMA) copolymer and surface crosslinking of these NPs,
- Examination of the antibacterial activity and biocompatibility of all the materials produced.

4.1 Synthesis and Characterization of Quaternized Poly(4VP-co-OEGMA) Copolymer

The copolymer used in the coating of NPs was produced by free radical polymerization of 4VP and OEGMA monomers. The polymer obtained was characterized by FT-IR and NMR spectroscopies, and GPC.

The FT-IR spectrum of the poly(4VP-co-OEGMA) copolymer is given in Figure 4.1. In the spectrum, the pyridine ring in the 4VP monomer is characterized by both the bands at 1600 cm^{-1} and 1415 cm^{-1}, while the OEGMA monomer chemical structure is characterized via both bands at 1725 cm^{-1} and 1100 cm^{-1} which belong to the C=O group and the C–O–C ether groups in its side chain, respectively [106].

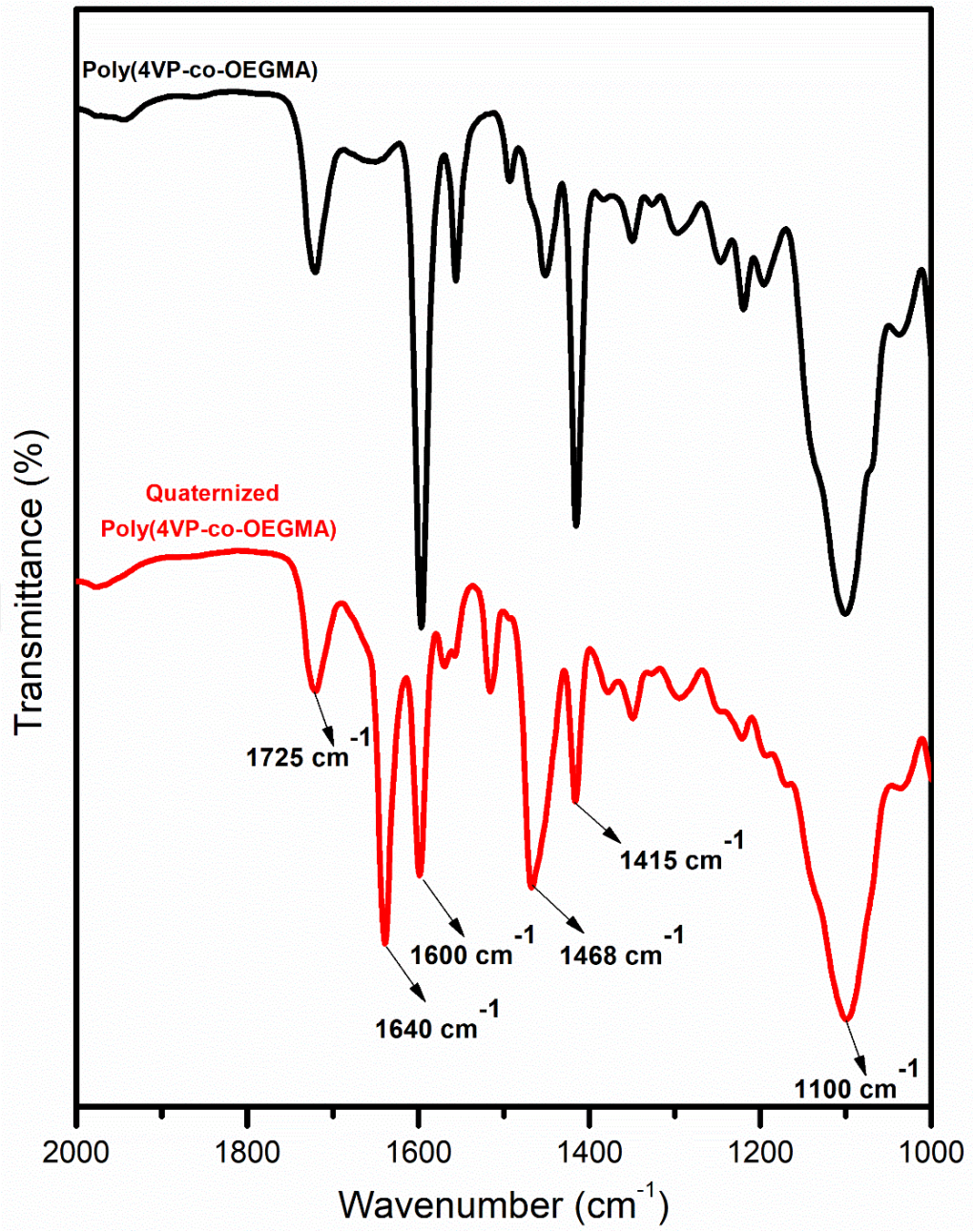


Figure 4.1 FT-IR spectra of poly(4VP-co-OEGMA) and the quaternized poly(4VP-co-OEGMA) copolymer

To analyze the chemical structure of the copolymer, NMR spectroscopy was also used. ^{1}H-NMR spectrum of the synthesized poly(4VP-co-OEGMA) copolymer is given Figure 4.2. At 8.26 and 6.59 ppm, the protons of pyridine rings are seen clearly, while the CH_2 protons on the side chain of OEGMA are observed at 3.50 ppm. The solvent peaks are also shown in the spectrum at 3.3 and 2.5 ppm for water and DMSO, respectively [106].

The monomer quantities in the poly(4VP-co-OEGMA) copolymer chain were determined from peak areas in the 1H-NMR spectrum. For this purpose, peak areas of pyridine rings (8.26 and 6.59 ppm) and OEGMA chains (3.50 ppm) were used. It was shown that 90 mol% of the monomers were 4VP and 10 mol% of the monomers were OEGMA monomers in the final copolymer chain, which are the same mole percentage of 4VP and OEGMA monomers used in the feed of polymerization. In addition, monomer peaks are not observed in the NMR spectrum, which indicates the successful removal of unreacted monomers.

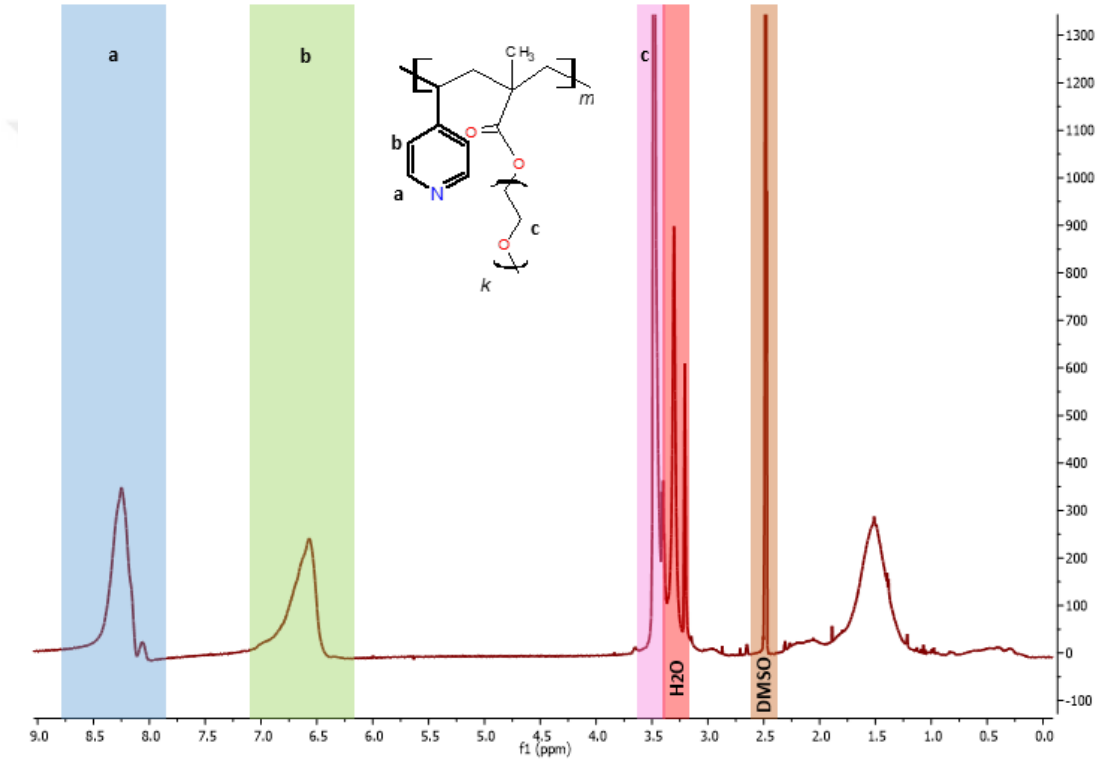


Figure 4.2 ^{1}H-NMR Spectrum of poly(4VP-co-OEGMA) copolymer in deuterated DMSO

The poly(4VP-co-OEGMA) random copolymer obtained was further analyzed using GPC to determine its purity, MW, and dispersity.

The chromatogram of poly(4VP-co-OEGMA) copolymer from the RI detector of the GPC is given in Figure 4.3. The unimodal peak eluted at 2.56 mL corresponds to the polymer, and the small positive and negative peaks between 3.2 and 3.9 mL are injection peaks observed in all chromatograms. As a result of the GPC analysis, the MW of the poly(4VP-co-OEGMA) copolymer was 29.9 kDa, and dispersity

Đ (M_W/M_n) was 1.4. The GPC analysis shows that the pure copolymer with unimodal distribution was produced.

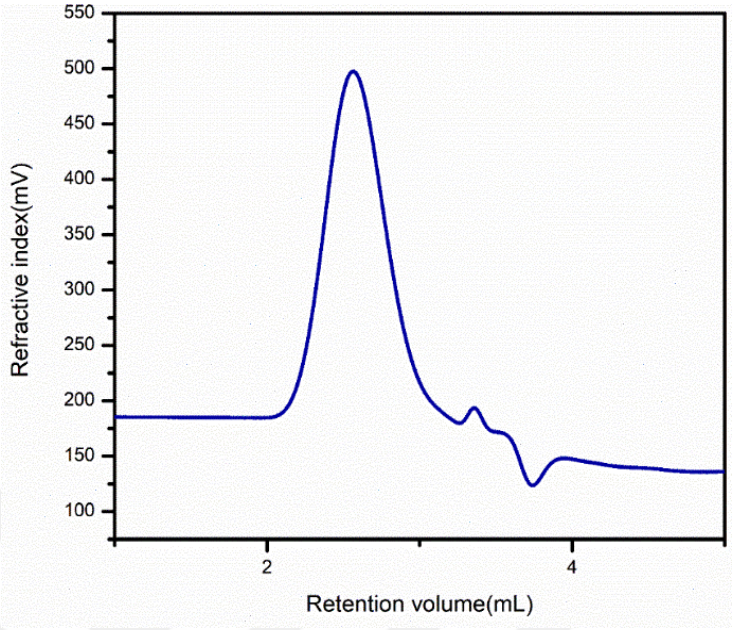


Figure 4.3 GPC chromatogram of poly(4VP-co-OEGMA) copolymer

FT-IR and ^{1}H-NMR spectroscopies, as well as GPC results reveal the successful production of the random poly(4VP-co-OEGMA) copolymer.

In the next step, the pyridine groups of the poly(4VP-co-OEGMA) copolymer were quaternized with BrH to obtain positively charged copolymer containing quaternary ammonium groups. FT-IR spectroscopy was used to determine the quaternization degree of the 4VP units in the polymer structure in the obtained cationic poly(4VP-co-OEGMA).

FT-IR spectrum of the quaternized poly(4VP-co-OEGMA) copolymer, given in Figure 4.1, allows to easily indicate the QD of 4VP rings. In the spectrum of quaterinezd poly(4VP-co-OEGMA) copolymer, new bands are observed at 1640 cm^{-1} and 1468 cm^{-1} [106]. These two peaks belong to the quaternized pyridine rings. Using Equation 3.1 [106], the ratio of the absorbances of both the 1600 cm^{-1} and 1640 cm^{-1} peaks gives the degree of quaternization in the copolymer chain as 42%. According to the Gokkaya et al. study [43], if the QD of pyridine rings is between 30% and 50%, this polymer has the maximum antibacterial activity, however, outside this range the antibacterial activity decreases, which is related to the hydrophobicity and hydrophilicity ratio.

The size, and zeta potential of quaternized poly(4VP-co-OEGMA) copolymer were also analyzed by DLS and ELS spectroscopy. As a result, the hydrodynamic diameter of polymer was 3.5 nm and PdI=0.55 with zeta potential of +10.8 mV.

4.2 Synthesis and Characterization of Polycationic Coated NPs

At first, PLGA NPs were prepared using 0.5 mg/mL of PLGA via the nanoprecipitation technique. The PLGA NP solutions obtained were characterized by FT-IR, DLS, and ELS spectroscopies, as well as SEM.

The structure of PLGA NPs was confirmed by the FT-IR spectrum (Figure 4.4). Figure 4.4 represents the characteristics of the PLGA NP bands at 1749 cm^{-1}, 1165 cm^{-1}, and 1085 cm^{-1}. The strong sharp band at 1749 cm^{-1} belongs to ester bond (C=O), while bands between 1165 cm^{-1} and 1085 cm^{-1} belong to C–O bond. In addition, the bands of the C–H stretch of CH_2, and C–H stretch of –C–H– at 2993 cm^{-1} and 2989 cm^{-1} respectively were also observed. This indicates the PLGA structure in the formed NPs [113].

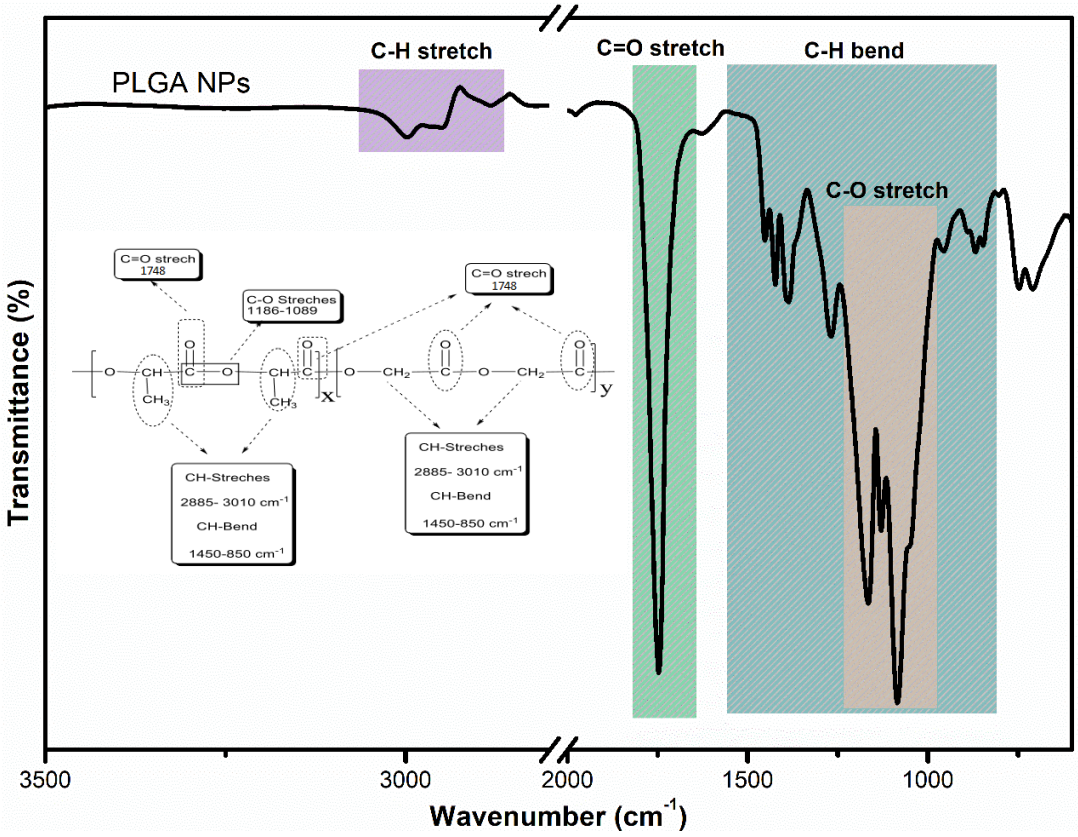


Figure 4.4 FT-IR spectrum of PLGA NP

The hydrodynamic diameter, hydrodynamic size distribution, and zeta potential of PLGA NPs were also analyzed by DLS and ELS spectroscopy. Figure 4.5 shows the size distribution of the PLGA NPs by intensity, with a hydrodynamic diameter of 129 nm (Table 4.1). Table 4.1 also shows that the PdI of PLGA NPs is 0.07, which is close to zero, indicating that PLGA NPs are monodisperse and did not form larger aggregates during NP formation. In addition, PLGA NPs have a zeta potential of -28 mV.

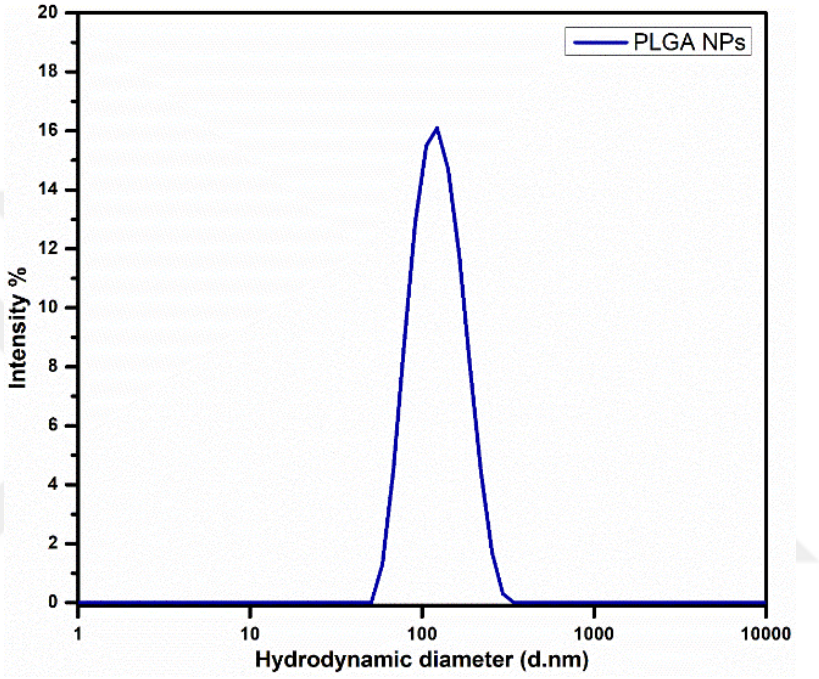


Figure 4.5 Hydrodynamic size distribution of PLGA NPs

In the next step, polycationic NC-NPs with different sizes were produced by adding different concentrations of quaternized poly(4VP-co-OEGMA) to a constant concentration of PLGA NP solutions (0.5 mg/mL). The prepared polycationic NC-NPs were characterized by FT-IR, DLS, and ELS spectroscopies, and SEM. Furthermore, the amount of unbound polymer in the NP solutions was determined using GPC.

The structures of the produced polycationic NC-NPs (NC1, NC2, NC3, NC4, NC5, NC6, NC7, and NC8) were confirmed by FT-IR spectra (Figure 4.6). FT-IR spectra were also used to determine QD%.

The characteristic bands of the pyridine rings of 4VP (1600 cm-$^{-1}$, 1640 cm^{-1}, 1468 cm^{-1}, and 1415 cm^{-1}) and the characteristic bands of OEGMA (1725 cm^{-1}, and 1100 cm^{-1}) can be seen in all spectra (Figure 4.6).

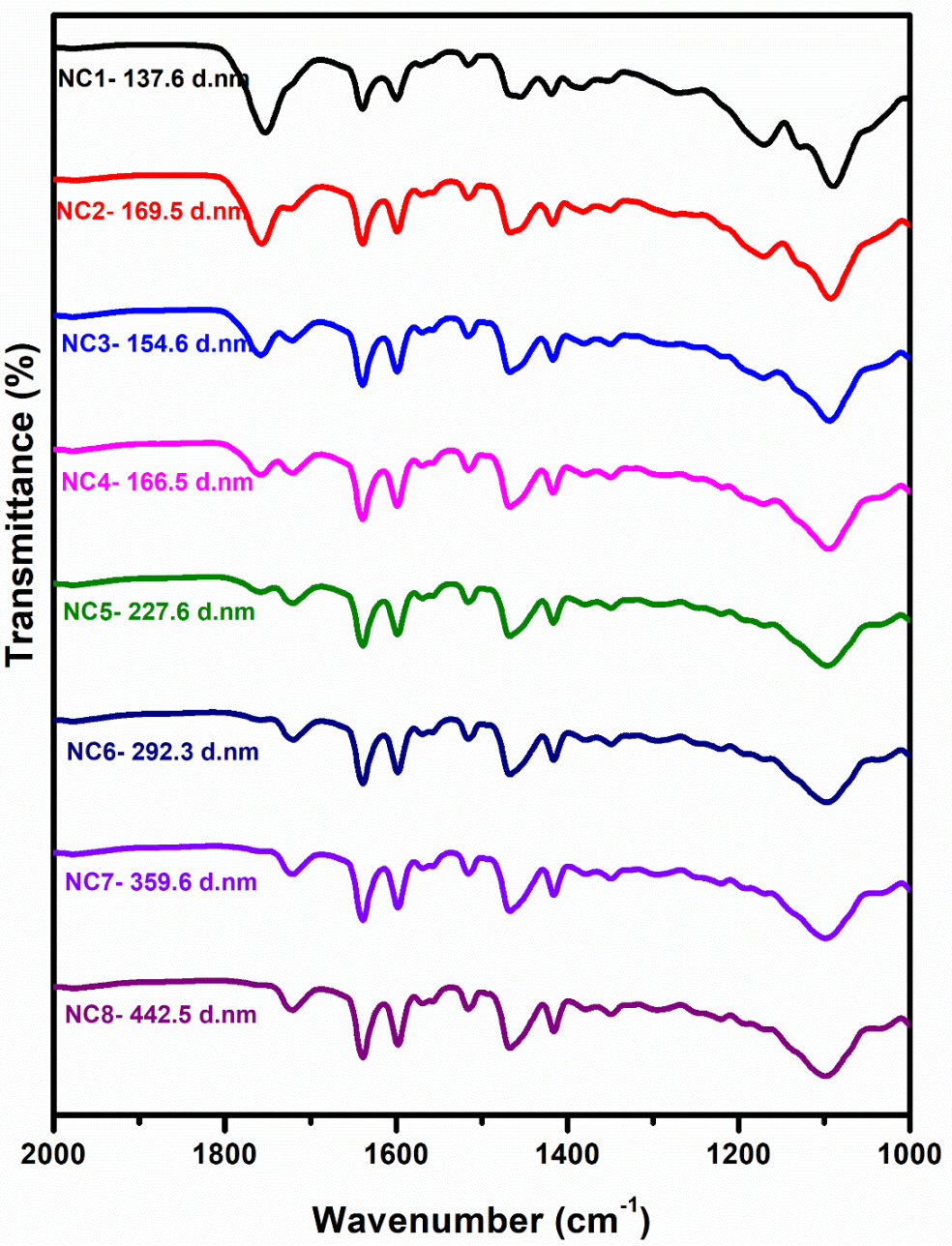


Figure 4.6 FT-IR spectra of polycationic NC-NPs

On the other hand, the intensity of the characteristic peaks of PLGA decreases with the concentration of quaternized poly(4VP-co-OEGMA) in Figure 4.6, and the peaks of PLGA almost disappear at the highest polycation concentrations. As shown in Figure 4.7, the characteristic peaks of PLGA NPs (1749 cm^{-1}, 1165 cm^{-1},

and 1085 cm^{-1}) were not observed in the spectrum of NPs with the highest polycations concentration (NC8) compared to the spectrum of NPs with the lowest polycations concentration (NC1). This proves that PLGA NP is partially coated at lower polycation concentrations, while the surface of the NP is almost saturated with the polycation at high polycation concentrations [114].

The quaternization degree values of NC-NPs were calculated using Equation 3.1 and determined as 42%, which is the same as the polycations' quaternization degree (Table 4.1).

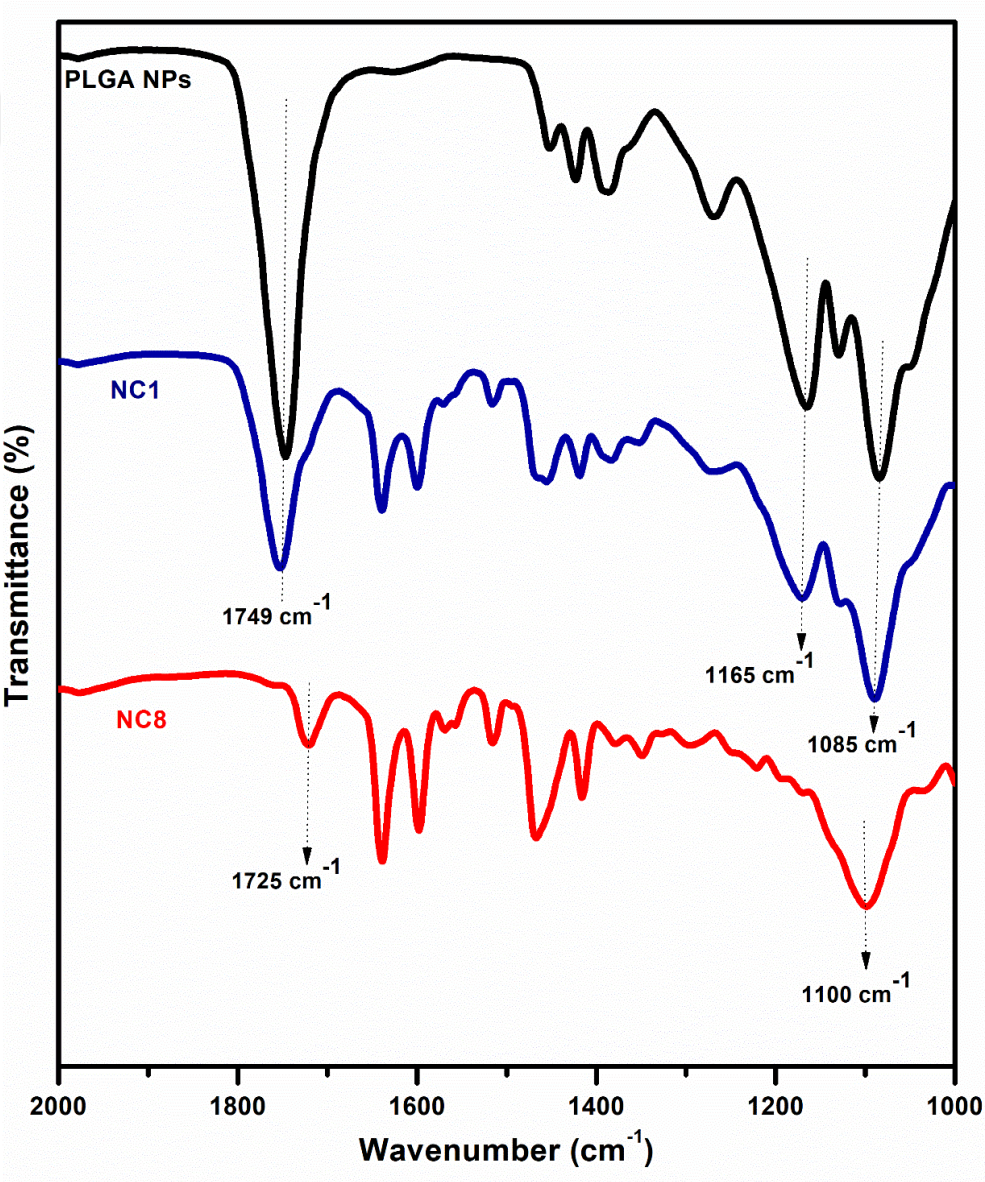


Figure 4.7 FT-IR spectra of PLGA , NC1, and NC8 NPs

The hydrodynamic diameter, hydrodynamic size distribution, and zeta potential of the produced NC-NPs were analyzed by DLS and ELS spectroscopy.

Figure 4.8 reveals the size distribution of the polycationic NC-NPs by intensity. This figure shows that there was a unimodal size distribution in the first four concentrations (NC1, NC2, NC3, and NC4), which indicates that there was no aggregation of NPs. In contrast, in the higher concentrations of quaternized poly(4VP-co-OEGMA), as in (NC5, NC6, NC7, and NC8), a second peak appeared, indicating that there were a number of aggregates [115].

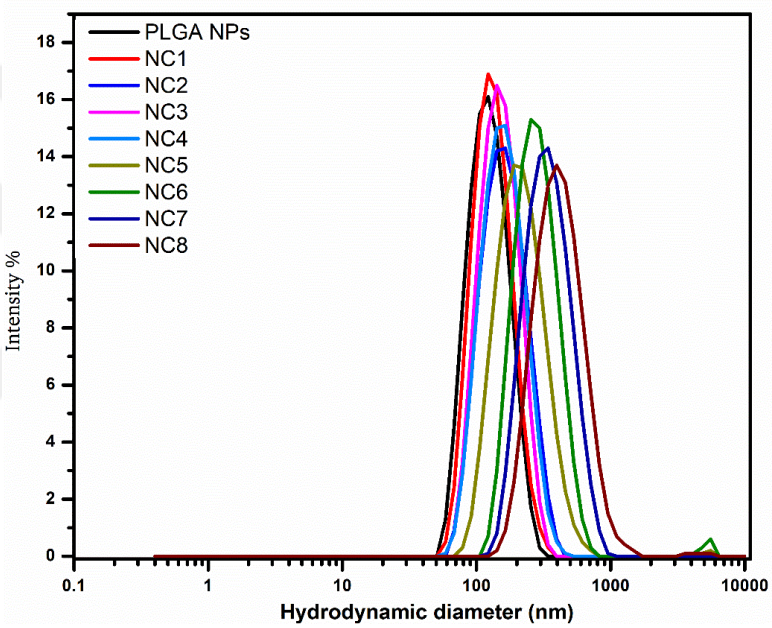


Figure 4.8 Polycationic NC-NPs' size distribution by %-Intensity

Figure 4.9 shows the change in physicochemical properties of NC-NPs as a function of polycation concentration; as quaternized poly (4VP-co-OEGMA) concentration increases, their hydrodynamic diameter increases as well and varies linearly from 138 to 443 nm (Table 4.1). Their polydispersity index (PdI) ranged between 0.094 and 0.249 (Table 4.1), which is below 0.3 indicating a narrow size distribution [116]. In addition, NPs are positively charged after coating with a polycation, with zeta potential values within the range of +35 mV and +56.4 mV (Table 4.1). Since quaternized poly(4VP-co-OEGMA) interacts electrostatically with negatively charged PLGA NPs, this shows that PLGA NPs were successfully coated and positively charged NC-NPs were produced.

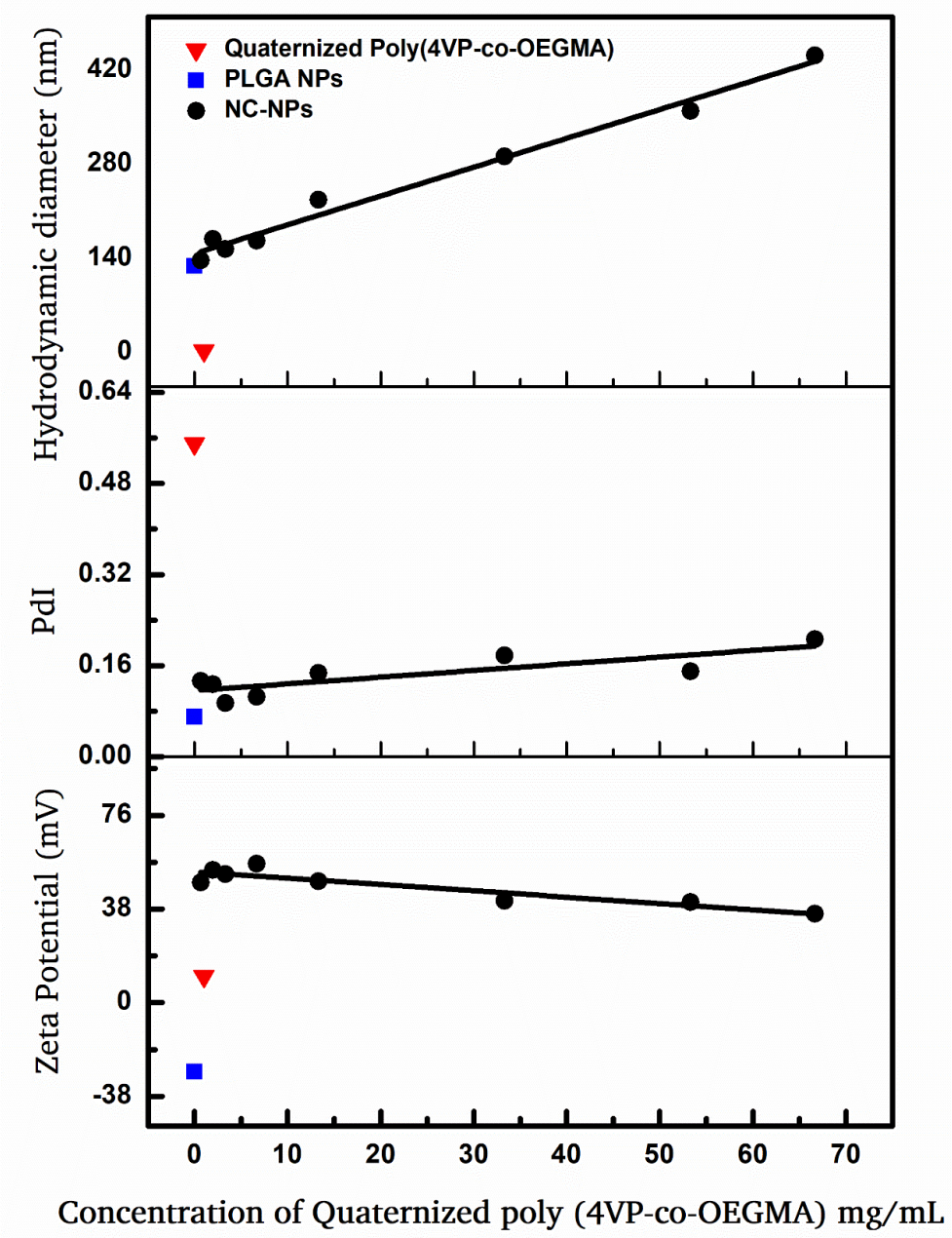


Figure 4.9 The hydrodynamic diameter, zeta potentials and polydispersity indices of NC-NPs depending on the concentration of quaternized poly(4VP-co-OEGMA)

The ZetaSizer-Ultra was also used to count the number of polycationic NC-NPs. All prepared NP solutions were diluted to obtain equal polycation concentrations (1 mg/mL) in each sample before measurement of the number of NPs (Figure 4.10). The results revealed that the number of NPs ranges between 5.47×10^8 and 458×10^8 (Table 4.1).

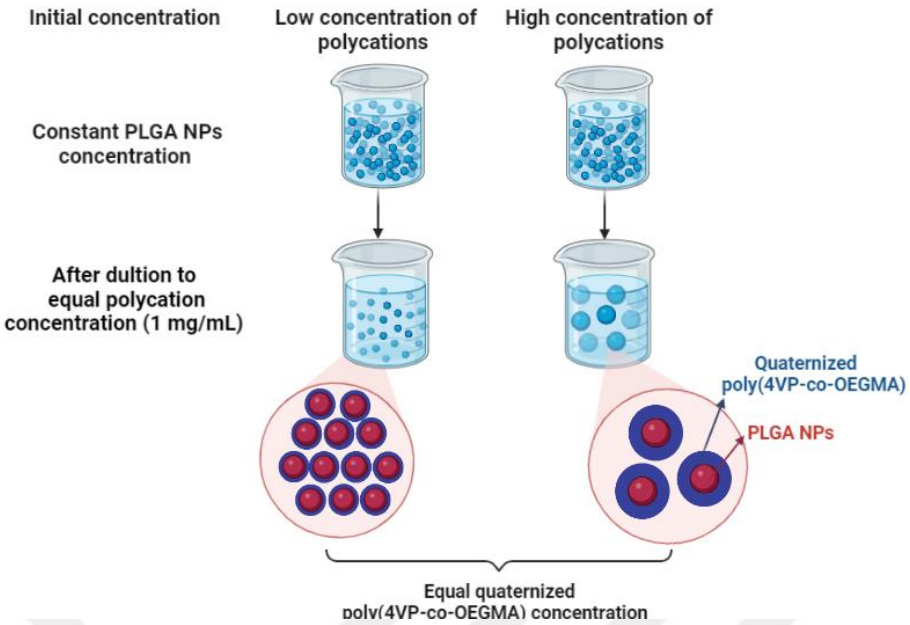


Figure 4.10 Schematic representation of the number of NPs in the NPs solutions after diluting to equal polycations concentration (1mg/mL)

Figure 4.11 shows the number of produced NPs as a function of their initial polycation concentration. The NPs' numbers significantly decline as the initial concentration of quaternized poly (4VP-co-OEGMA) increases.

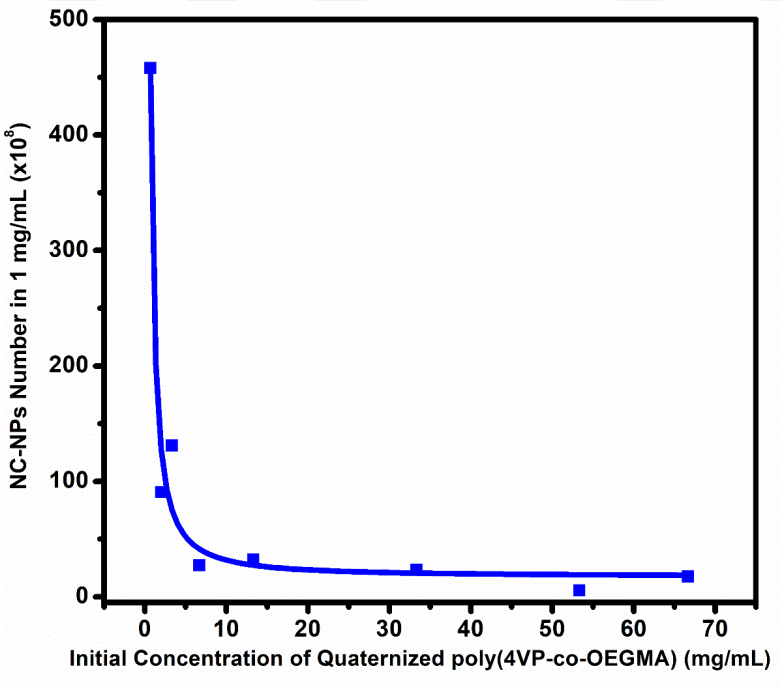


Figure 4.11 Count of NC-NPs diluted to equivalent (1mg/mL) concentration of quaternized poly(4VP-co-OEGMA) depending on the initial concentration of polycation

The spherical morphologies of the dried NPs were confirmed by SEM images (Figure 4.12). The size of PLGA, NC1, NC3, and NC7 were obtained as ~101, 121, 146, 187 nm in diameter, respectively.

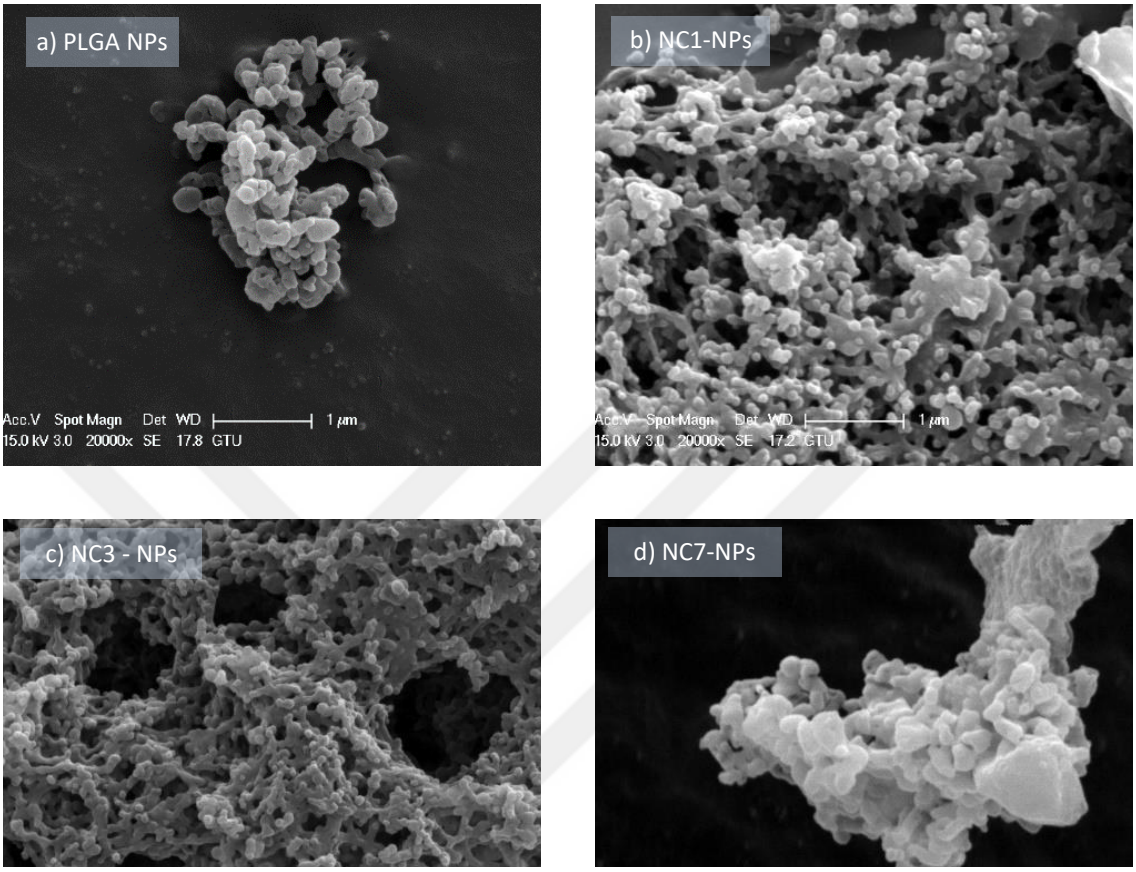


Figure 4.12 SEM images of PLGA NPs(a), NC1-NPs(b) NC3-NPs(c), and NC7-NPs(d) showed spherical morphologies at 20.000X magnification

Then, the surface groups of these NPs were crosslinked to stabilize the structure and study the crosslinking effect. The same quantity of DBH (1.2 µL) was added to all polycationic NC-NPs, and the reaction was carried out at 70°C for 24h. The obtained surface crosslinked polycationic NPs (SC-NPs) were characterized by FT-IR, DLS, and ELS spectroscopies.

The structure of the produced polycationic SC-NPs (C1, C2, C3, C4, C5, C6, C7, and C8) and their quaternization degrees QD% were investigated using FT-IR spectra (Figure 4.13).

In Figure 4.13, all spectra show that the structure of the NPs after crosslinking of surface groups did not change, and the characteristic bands of the pyridine rings

of 4VP and OEGMA are clearly observed. The quaternization degree of polycationic SC-NPs was calculated using Equation 3.1 between 44% and 46.7% (Table 4.1).

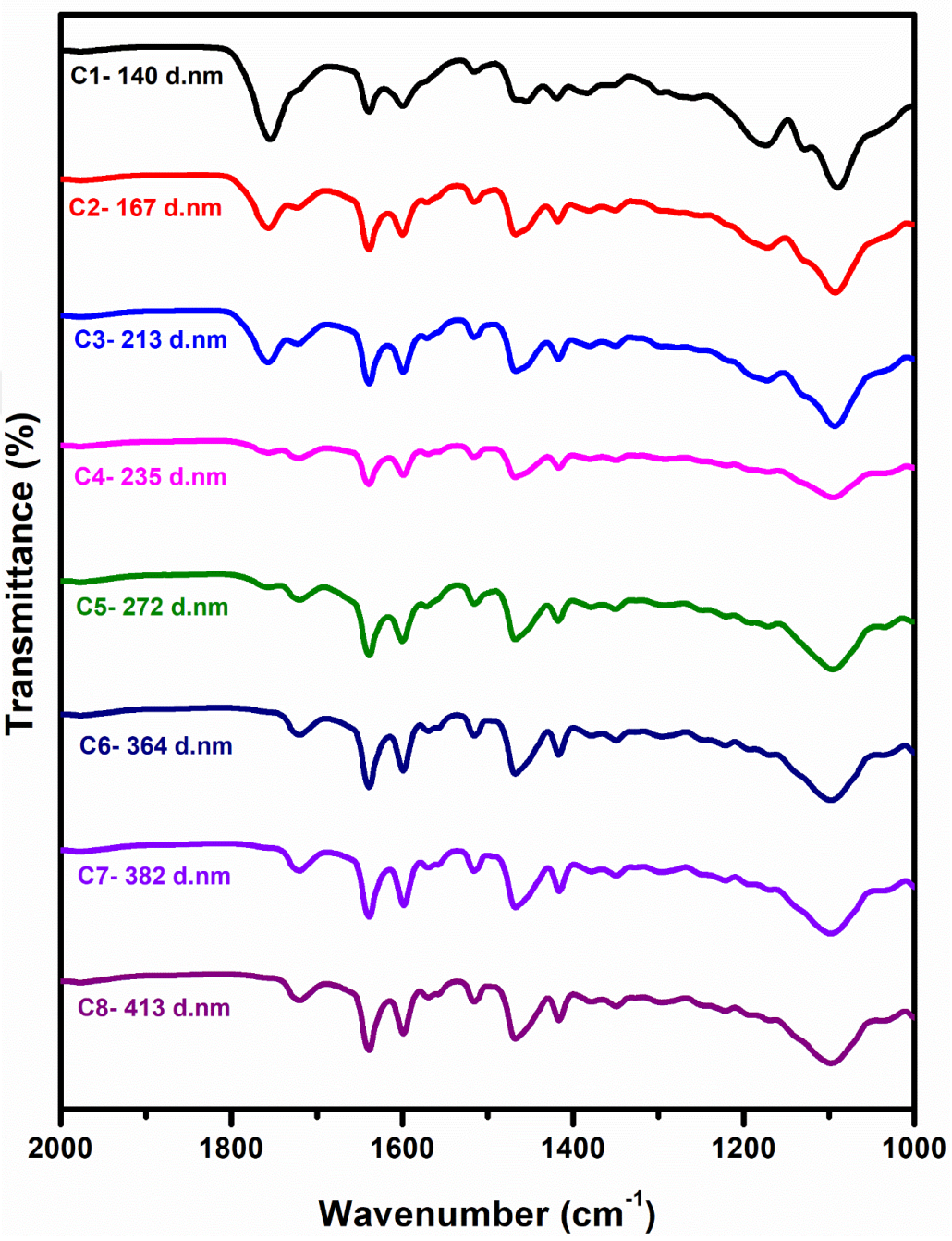


Figure 4.13 FT-IR spectra of polycationic SC-NPs

In addition, the hydrodynamic diameter, hydrodynamic size distribution, and zeta potential of the produced NPs after surface crosslinking were analyzed by DLS and ELS spectroscopy.

Figure 4.14 represents the size distribution of the NPs after the surface crosslinking by intensity. As for the NPs before surface crosslinking, Figure 4.14 shows that there was one peak in the first two concentrations (C1, and C2) after surface crosslinking, which indicates that there was no aggregation in the particle solutions. In contrast to NPs before crosslinking, a second peak was observed in all NPs of C3, C4, C5, C6, C7, and C8, which could be due to DBH also increases secondary aggregation.

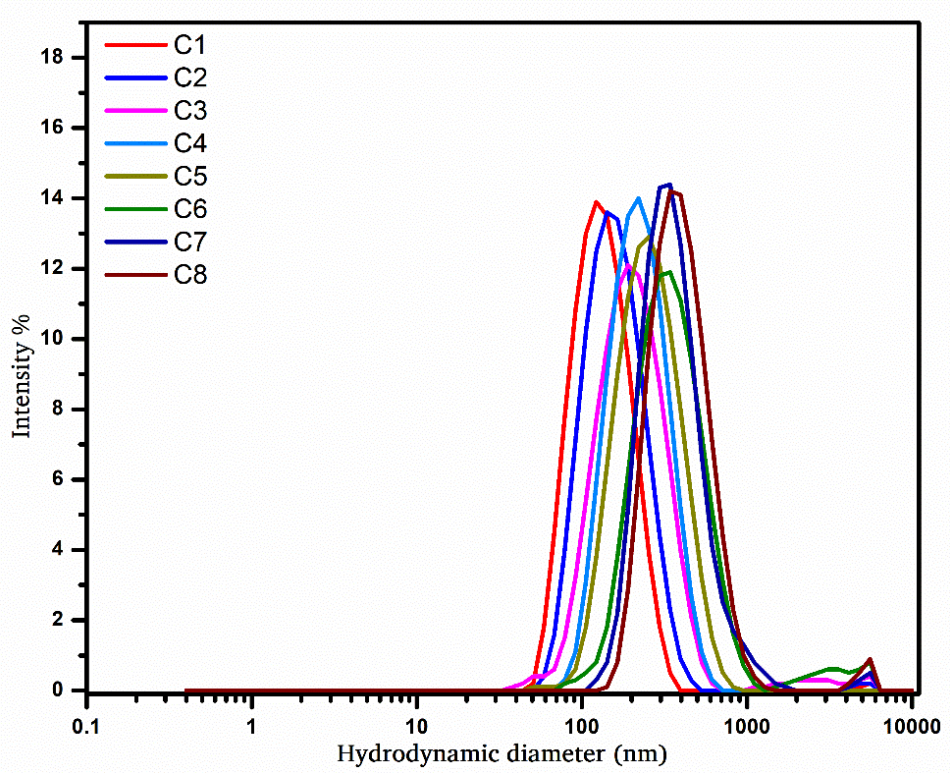


Figure 4.14 Polycationic SC-NPs' size distribution by %-Intensity

Figure 4.15 shows the change in physicochemical properties of polycationic SC-NPs as a function of polycation concentration by comparing with NC-NPs. The hydrodynamic diameter of NPs after crosslinking ranged between 139.6 and 412.7 nm (Table 4.1). Polycationic SC-NPs have a PdI between 0.136 and 0.249 (Table 4.1), which is below 0.3, indicating a narrow size distribution. The zeta potential values of SC-NPS were within the range of +44.0 mV and +46.7 mV (Table 4.1).

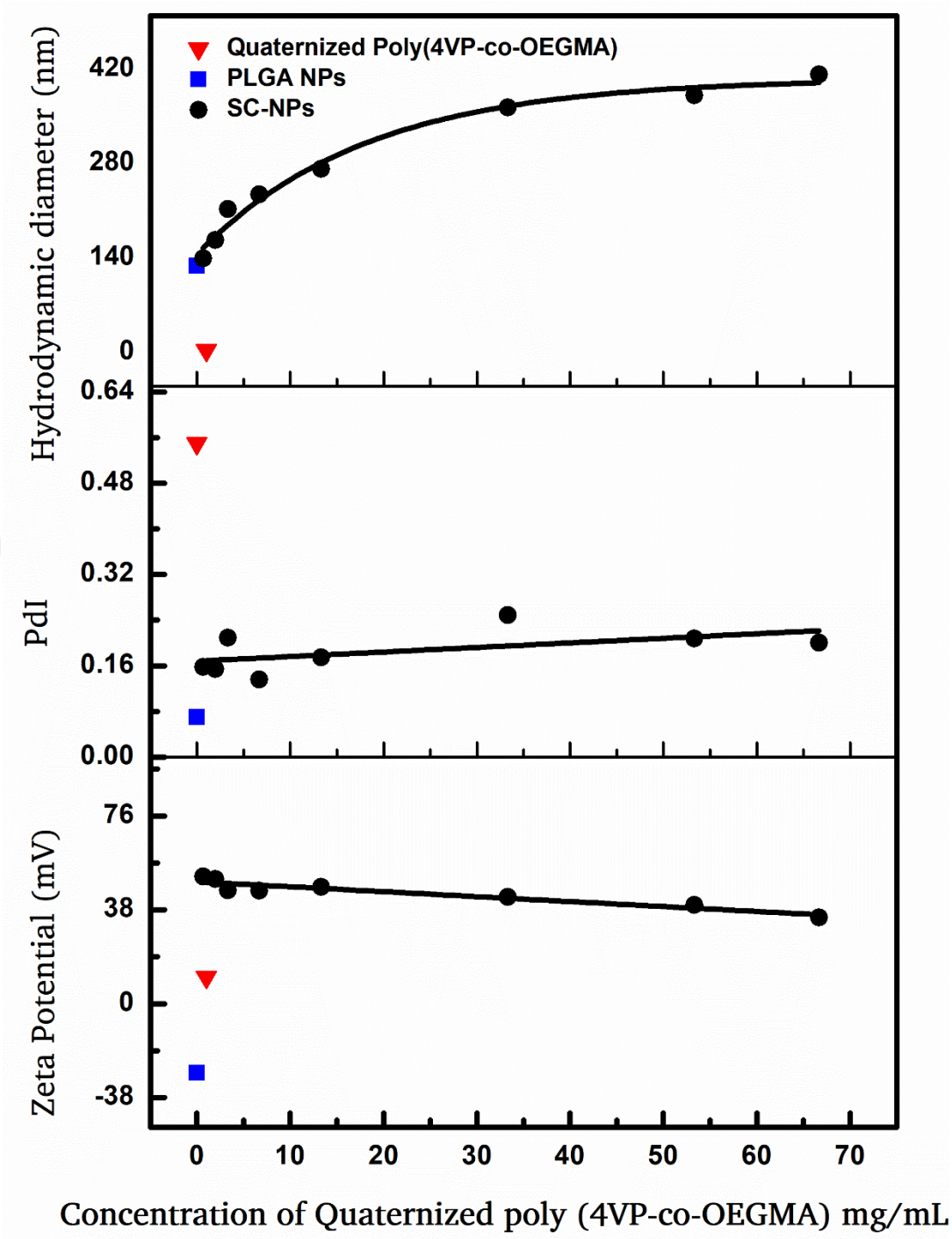


Figure 4.15 The hydrodynamic diameter, zeta potentials and polydispersity indices (PDI) of polycationic SC-NPs depending on the concentration of quaternized poly(4VP-co-OEGMA)

Table 4.1 Hydrodynamic diameters (D), polydispersity index (PdI), zeta potentials (ζ_P), quaternization degrees (QD), and counts of NPs

Sample	PdI	z-Average D (nm)	Intensity based D (nm)	ζ_P (mV)	QD (%)	NPs Number in 1mg/ml (x10^8)
PLGA	0.070	115.8	129.0	-28.0	-	-
NC1	0.133	126.2	137.6	48.8	42.3	458
NC2	0.127	149.6	169.5	53.9	42.7	90.5
NC3	0.094	138.9	154.6	52.2	42.5	131
NC4	0.105	147.1	166.5	56.4	42.4	27.2
NC5	0.147	196.9	227.6	49.3	42.4	32.1
NC6	0.178	267.2	292.3	41.3	42.8	23.3
NC7	0.150	312.2	359.6	40.8	42.5	5.47
NC8	0.206	381.1	442.5	36.0	42.5	17.5
C1	0.158	123.6	139.6	51.5	44.0	-
C2	0.154	145.5	167.1	50.4	45.4	-
C3	0.209	184.8	212.6	45.9	46.2	-
C4	0.136	201.6	234.4	45.8	46.7	-
C5	0.175	230.6	272.4	47.3	45.5	-
C6	0.249	324.8	363.5	43.2	45.8	-
C7	0.208	336.8	381.9	40.0	45.9	-
C8	0.200	375.6	412.7	34.9	45.5	-

Since the binding of poly(4VP-co-OEGMA) on the PLGA NP surface is adsorption depending on electrostatic interactions, determining the isotherm of the adsorption can give information about the process. For this purpose, bound and unbound polymer concentrations have been determined by analyzing and quantifying the free polymers in NP solutions using GPC. GPC was applied for NC1, NC3, NC5, and NC7 NPs samples.

Concentrations of bound (CB) and unbound (CU) polycations were plotted as linear, Langmuir, and Freundlich models in Figure 4.16 to evaluate the adsorption mechanism. The regression coefficient was the highest (R2=0.9892) for the linear adsorption isotherm, which reveals that the adsorption mechanism between polycation and PLGA fits best with the linear isotherm. It is known that the linear isotherm is suitable for very dilute solutions, which indicates that there are more room for the potential adsorption of polycations on the PLGA surface.

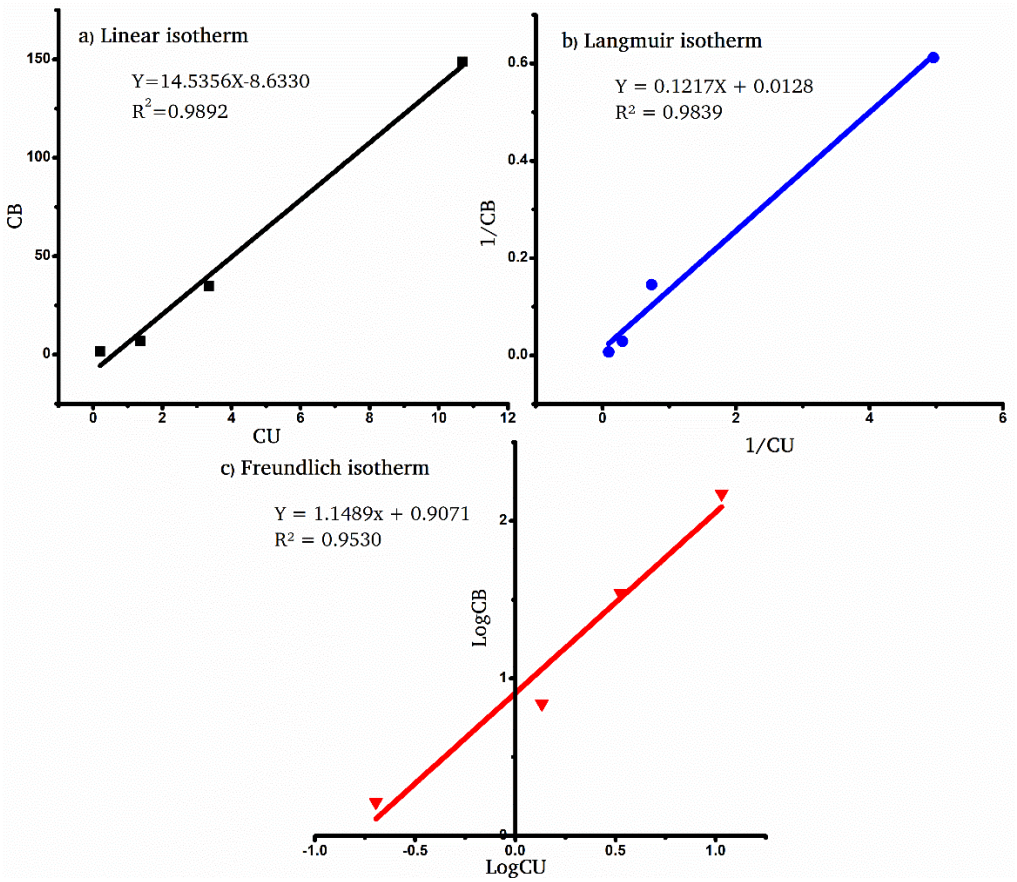


Figure 4.16 Linear (a), Langmuir (b), and Freundlich (c) adsorption of CN1, CN3, CN5, and CN7 NPs

4.3 In-Vitro Tests

4.3.1 Antibacterial activity assay

Using the broth microdilution method, the antibacterial activity of quaternized poly(4VP-co-OEGMA) copolymer, NC-NPs, and SC-NPs was investigated against *E. coli* and *S. aureus* bacteria. All materials were examined for polycation concentration within the range of 4–512 μg/mL.

MIC values for all samples obtained from broth microdilution analysis are given in Table 4.2. As seen in the table, polycation has the MIC values of 8 μg/mL and <8 μg/mL against *E. coli* and *S. aureus*, respectively.

The nanoparticles with the lowest concentration of quaternized poly(4VP-co-OEGMA) exhibited the highest MIC values against the bacteria. The MIC values against *E. coli* for NC1 and C1 samples were 32 μg/mL and 16 μg/mL, respectively, while MIC values against *S. aureus* for NC1 and C1 samples were 16 μg/mL. This can be due to the partial coating of these NPs with the polycation.

When the concentration of polycation increases, the MIC values of NC-NPs and SC-NPs decrease to the value of 8 μg/ml against both bacteria. 8 μg/ml is the same MIC value of polycation against *E. coli*, while this value is higher than the MIC value of polycation against *S. aureus*. It is revealed that the bulk quaternized poly (4VP-co-OEGMA) has the highest antibacterial efficiency compared to the MIC values of its surface coated NPs. This can be attributed to that the movement of polycations on the surface of NPs are restricted compared to the free polymer chains which reduces the possible interactions with the surface of the bacteria.

As mentioned before, Kadayifci et al. produced three different charged of cationic poly(4VP-b-OEGMA) core-crosslinked micelles. These micelles showed comparable antibacterial activity against *E. coli* with an inhibitory effect with MIC values of 0.6 mg/mL at their maximum concentration, and there was no antibacterial activity against *S. aureus.* Moreover, it was found that these polycationic micelles have long-term stability with activity against gram-negative bacteria [15]. This study showed that both NC-NPs and SC-NPs have much better

antibacterial activity against both *E. coli* and *S. aureus* compared to the Kadayifci et al. study.

Table 4.2 MIC values of quaternized poly(4VP-co-OEGMA), NC-NPs, and SC-NPs

Quaternized poly (4VP-co-OEGMA) - MIC values (μg/mL)					
E.coli			*S.aureus*		
8			<8		
NC-NPs – MIC values (μg/mL)			SC-NPs -MIC values (μg/mL)		
Sample	*E.coli*	*S.aureus*	Sample	*E.coli*	*S.aureus*
NC1	32	16	C1	16	16
NC2	8	<16	C2	8	16
NC3	8	8	C3	8	8
NC4	8	16	C4	8	8
NC5	8	8	C5	8	8
NC6	8	<16	C6	8	8
NC7	8	8	C7	8	8
NC8	8	8	C8	8	8

MIC values in Table 4.2 are given as the polycation concentrations used in the NP preparation, and a correlation between MIC and NP size is not observed. To better evaluate the effect of size on the antibacterial activity, particle numbers of NPs are measured for a constant polycation concentration. Table 4.1 gives the particle numbers of NC-NPs diluted to 1 mg/mL polycation concentration. As seen from the table, the number of particles significantly decreases with the size of the NP. By using these particle numbers, the number of NPs that interact with the bacteria can be easily determined by dividing the particle number by the bacteria number, which is given as the MOI in bacteriophage studies to find the number of phages

infecting the bacteria. Therefore, we used the same parameter to reveal the effect of particle number on antibacterial activity.

By looking at MIC values, the size did not influence the antibacterial activity, but the number of particles changed depending on the polycation concentration because, in all samples, the same concentration of PLGA NP was coated with different concentrations of quaternized poly(4VP-co-OEGMA), but for MIC, an equivalent polycation NPs concentration was applied. MOI values were calculated according to Equation 3.2.

It is very clear that the MIC values may not have changed, however (Table 4.3) the number of NPs attached to the bacterial surface drastically decreases (Figure 4.17-18), showing that NP counts are directly related to their antibacterial activity.

Table 4.3 MOI values of NC-NPs

NC-NPs' MOI values		
Codes	*E.coli*	*S.aureus*
NC1	2290	1145
NC2	113	< 226
NC3	164	164
NC4	34	34
NC5	40	40
NC6	29	< 58
NC7	7	7
NC8	23	23

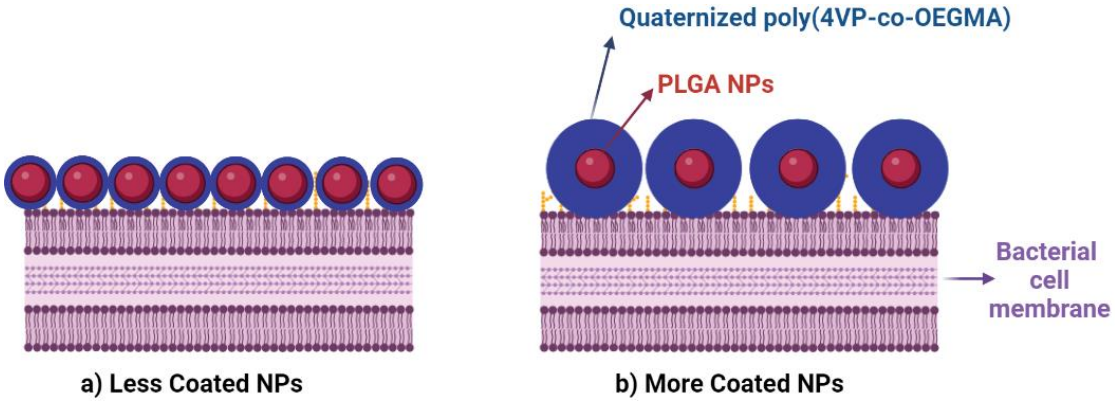


Figure 4.17 Schematic representation of number of NPs attached to the bacterial surface

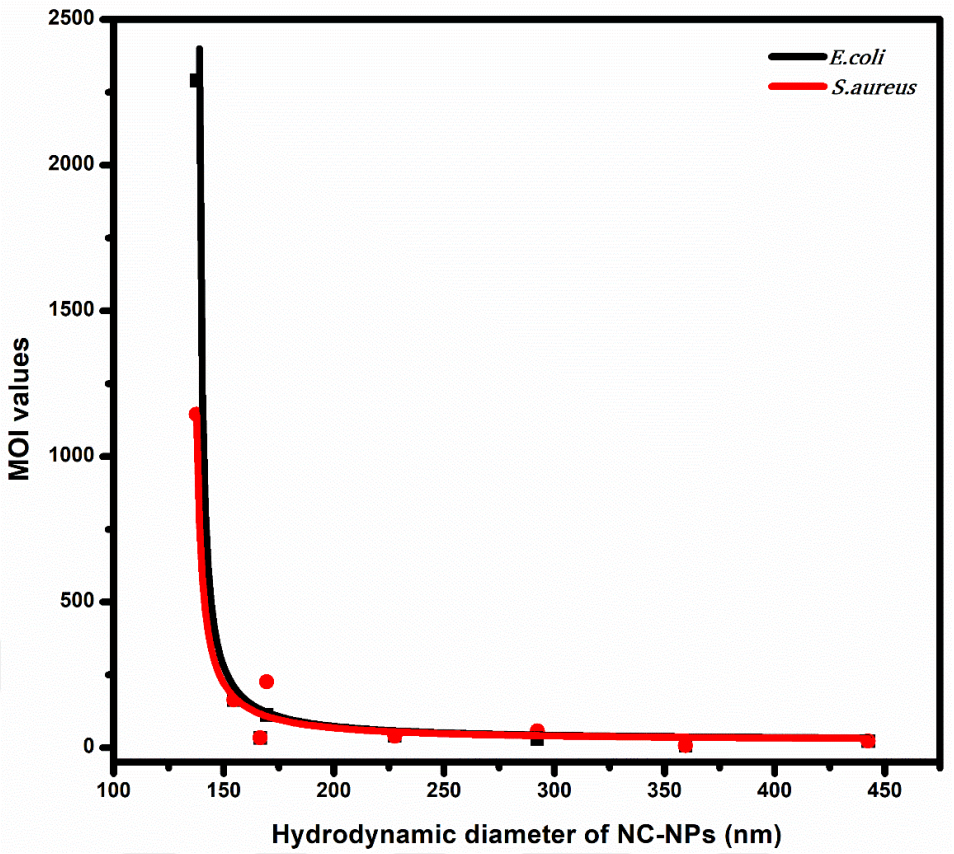


Figure 4.18 MOI values as a function of the hydrodynamic diameter of NC-NPs

4.3.2 Biocompatibility test

The cytotoxicity of the produced NPs was examined with the MTT method on L929 fibroblast cells using different concentrations (4, 8, 16, 32, 64, and 128 μg/mL) and using quaternized poly (4VP-co-OEGMA) copolymer as a control. Cell viability of produced NPs was using Equation 3.3. Figures 4. 19-20 show that all the produced NC-NPs and SC-NPs were biocompatible, having cell viability above 80%, when their concentration was below 32 µg/mL, while high-concentrated samples show less biocompatibility, having cell viability below 70%. As a result, all NPs were biocompatible with L929 fibroblasts in concentrations above their MIC values.

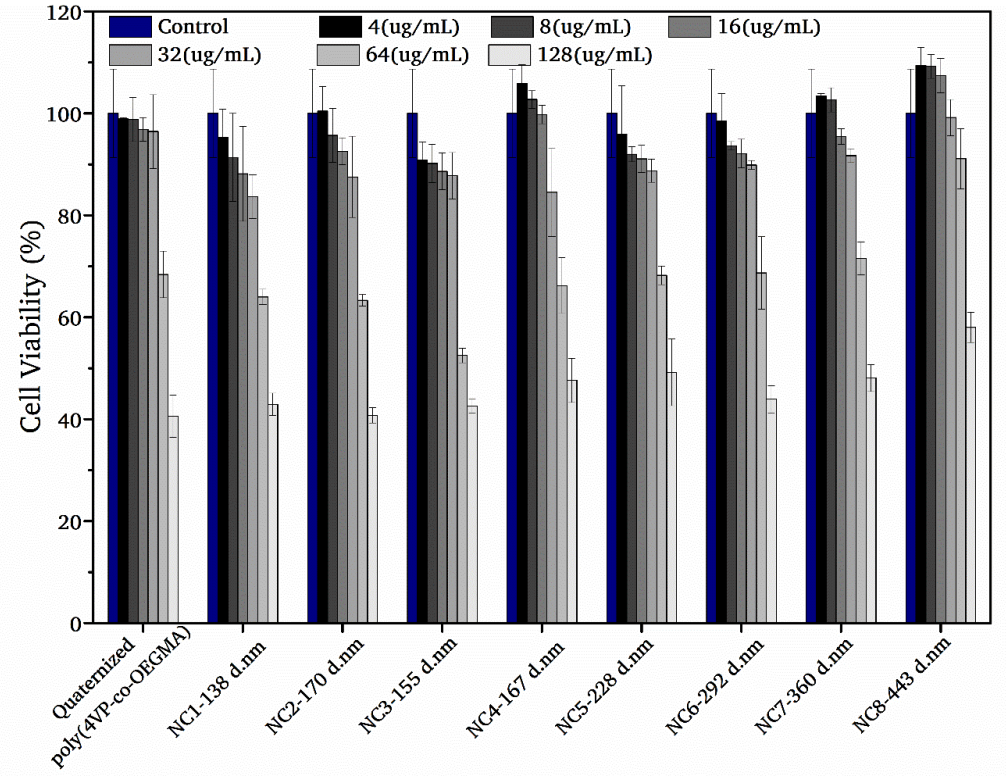


Figure 4.19 Effect of quaternized poly(4VP-co-OEGMA) copolymer, and NC-NPs on L929 fibroblast cell viability

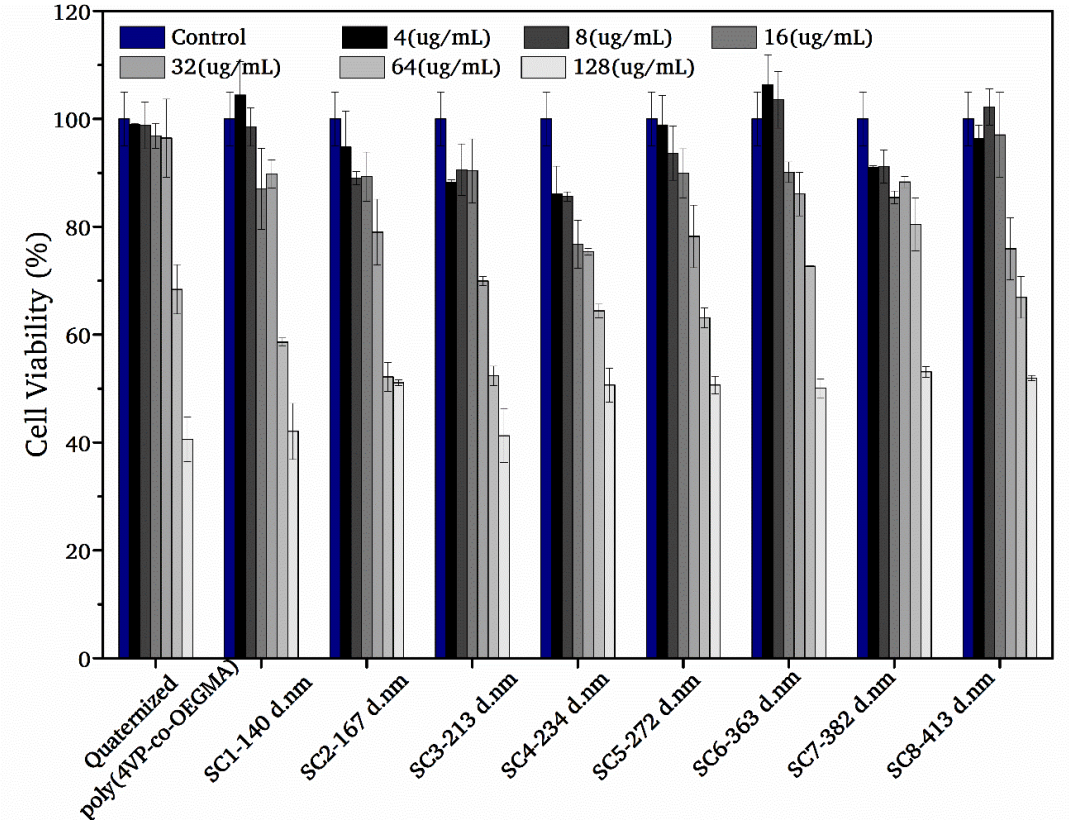


Figure 4.20 Effect of quaternized poly(4VP-co-OEGMA) copolymer, and SC-NPs on L929 fibroblast cell viability

IC_{50} values of the produced materials on fibroblast cells were calculated and shown in Table 4.4.

Table 4.4 illustrates that the IC_{50} of quaternized poly(4VP-co-OEGMA) copolymer was 108.89, NC-NPs were ranging between 104.05 and 122.84 , and SC-NPs were between 94.11 and 148.86

Table 4.4 IC_{50} values of quaternized poly(4VP-co-OEGMA) copolymer, NC-NPs, and SC-NPs in the group on L929 fibroblast cells

IC_{50} values of poly(4VP-co-OEGMA) (µg/mL)			
108.89			
Sample	**NC-NPs' IC_{50} values(µg/mL)**	**Sample**	**SC-NPs' IC_{50} values (µg/mL)**
NC1	111.06	**C1**	102.77
NC2	104.05	**C2**	111.42
NC3	100.60	**C3**	94.11
NC4	113.79	**C4**	124.49
NC5	122.84	**C5**	117.81
NC6	113.06	**C6**	122.64
NC7	120.11	**C7**	148.86
NC8	152.44	**C8**	133.60

Moreover, Figure 4.21 shows that IC_{50} values increased with the size of the NPs. In smaller NPs, it can be hypothesized that more particles interact with the cell membranes and disruption on the cell membrane occurs at more positions causing smaller IC_{50} value. However, in larger NPs, there are less number of particles in the solution and interacting with the cell membrane. Therefore, disruption on the cell membrane occurs at less number of positions which causes higher IC_{50} values that reveals that more particles are necessary to disrupt the cell membrane.

As a result, the concentration values showing the biocompatibility of quaternized copolymers, NC-NPs, and SC-NPs were obtained above the concentration values showing antibacterial studies. Accordingly, biocompatible polycations and all produced polycationic NPs that meet the criteria of the ISO 10993-5 standard and can be applied in biomedical fields have been successfully produced.

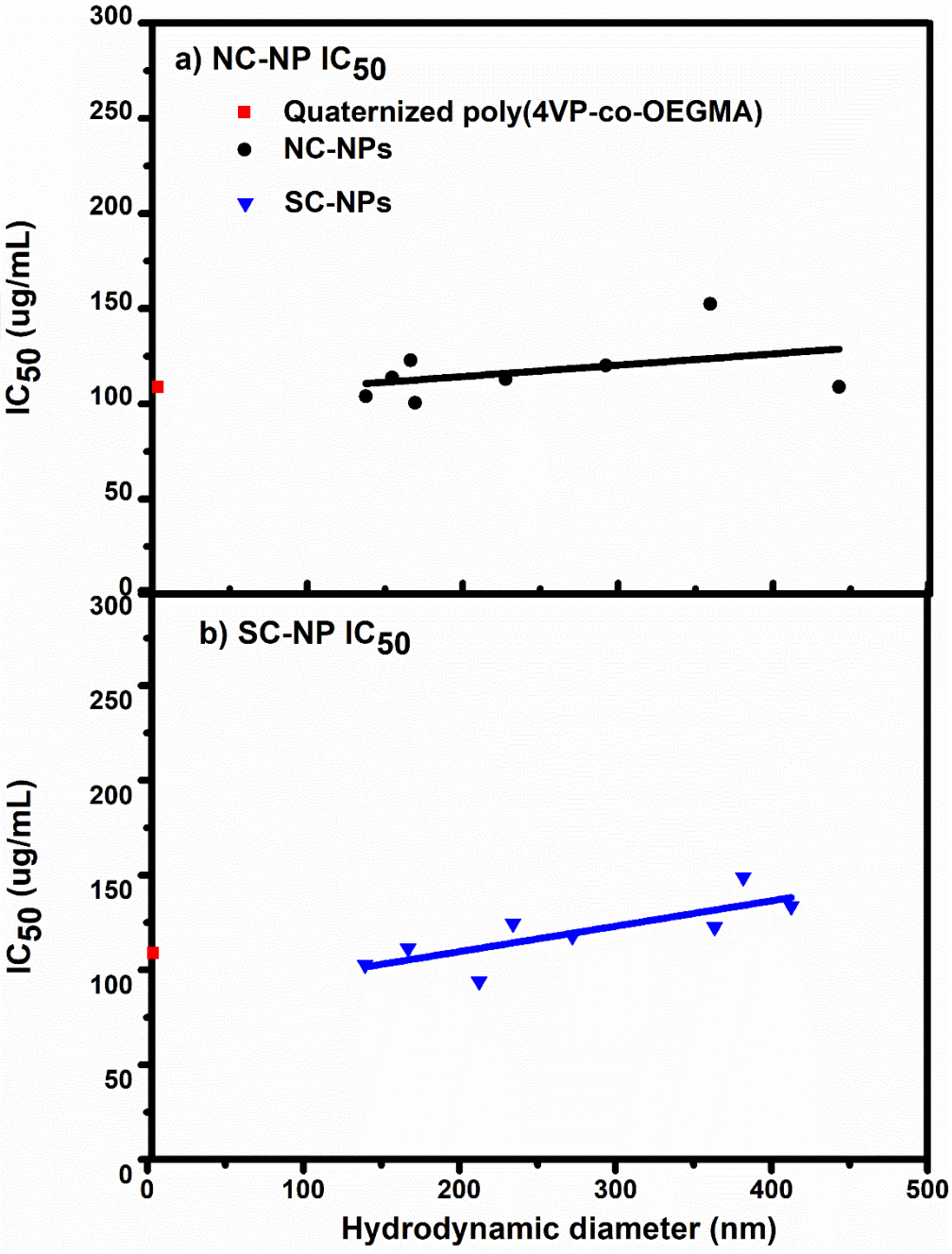


Figure 4.21 Half-maximal inhibitory concentration (IC_{50}) of quaternized poly(4VP-co-OEGMA) copolymer (red dot), NC-NPs (a), and SC-NPs (b) depending on the hydrodynamic diameter of the sample

4.4 CONCLUSION

In the thesis, differently sized inherently antibacterial NPs were produced, and their size-dependent antibacterial performance was assessed against both *E. coli* and *S. aureus* bacteria, as well as their biocompatibility on L929 fibroblast, was evaluated.

As a result of this study, the following conclusions were drawn:

- FT-IR and 1H-NMR spectroscopies, as well as GPC results, reveal the successful production of inherently antibacterial cationic poly(4VP-co-OEGMA) random copolymer.
- FT-IR, DLS, and ELS spectroscopy results revealed that the PLGA NPs were successfully produced with average hydrodynamic diameter of 129 nm and narrow size distribution.
- Different sizes of positively charged NPs were produced by coating a constant amount of PLGA NPs with different concentrations of quaternized poly(4VP-co-OEGMA). The characterization of NC-NPs revealed that as the poly(4VP-co-OEGMA) content increases, the surface PLGA NP becomes more saturated with the polycation. The hydrodynamic diameters of NPs increased linearly with polycation concentration from 138 to 443 nm with narrow size distribution and spherical morphology, and zeta potential values of NPs were between +35 and +56.4 mV.
- Surface groups of NPs were cross-linked with quaternization reaction successfully to stabilize their structure. The size of NPs slightly increased after cross-linking.
- Linear adsorption isotherm was observed in coating of NPs with the polycation, which indicates that there is more room on the surface of PLGA NPs for potential adsorption of poly(4VP-co-OEGMA).
- The antibacterial activity of the produced materials was investigated using the broth microdilution method against *E.coli* and *S.aureus* bacteria. MIC values showed that both NC-NPs and SC-NPs have antibacterial activity against both E. coli and S. aureus, which was much better than that in a previous study by our lab researchers, Kadayifci et al.

- The bulk quaternized polymer (4VP-co-OEGMA), on the other hand, exhibits the best antibacterial efficiency when compared to the MIC values of its surface-coated NPs. This could be explained by the fact that the mobility of polycations on the surface of NPs is constrained in comparison to the free polymer chains, which in turn lowers the possibility of contact with the bacteria's surface.
- MIC values of NPs were related to polycation concentration. When the number of particles of coated NPs was determined for these MIC values, it was revealed that NPs' numbers are directly related to their ability to kill bacteria since the number of particles attached to the bacterial surface drop sharply as particle size increases.
- The cytotoxicity of the produced polymeric materials was also investigated using the MTT method on L929 fibroblast cells. All NPs and the polymer itself were biocompatible on L929 fibroblast cells at concentrations above their MIC values with cell viability above 80%.
- IC50 values were calculated as well, and the result shows that more particles are necessary to disrupt the cell membrane because the IC50 values increased with the size of the NPs.

The results indicate that the inherent antibacterial activity and biocompatibility of the produced polycationic materials make them promising candidates for a variety of antibacterial applications. In addition, the fact that the NPs' antibacterial performance is size-dependent, allows to appropriately correlate structure-function relationship in antibacterial NPs and the development of more potent nanostructures for such purposes.

Future studies would involve crosslinking the surfaces of these NPs with varying concentrations of crosslinker and analyzing their antibacterial activity to better understand the impact of surface crosslinking on the antibacterial activity, coating the surfaces of the differently sized PLGA NPs with a constant content of polycations, and investigating their antibacterial activity. Furthermore, directly studying the effect of NPs' size on the antibacterial activity of the inherently antibacterial NPs without coating, which would give more clear and direct results.

Finally, the antibacterial efficacy of the produced polymeric materials could be examined against various species of bacteria.

REFERENCES

[1] P. Jt and A. As, '*Escherichia coli* and *Staphylococcus aureus*: leading bacterial pathogens of healthcare associated infections and bacteremia in older-age populations', *Expert Rev. Vaccines*, vol. 17, no. 7, Jul. 2018, doi: 10.1080/14760584.2018.1488590.

[2] F. Pahlevanzadeh *et al.*, 'A review on antibacterial biomaterials in biomedical applications: from materials perspective to bioinks design', *Polymers*, vol. 14, no. 11, p. 2238, May 2022, doi: 10.3390/polym14112238.

[3] M. Larry M. Bush FACP, Charles E. Schmidt College of Medicine, Florida Atlantic University, 'Overview of bacteria - infections', *MSD Manual Consumer Version*, Aug. 2022. https://www.msdmanuals.com/home/infections/bacterial-infections-overview/overview-of-bacteria?query=Overview%20of%20Bacteria (accessed Nov. 06, 2022).

[4] A. Singh and A. K. Dubey, 'Various biomaterials and techniques for improving antibacterial response', *ACS Appl. Bio Mater.*, vol. 1, no. 1, pp. 3–20, Jul. 2018, doi: 10.1021/acsabm.8b00033.

[5] W. Ma *et al.*, 'Ultra-efficient antibacterial system based on photodynamic therapy and co gas therapy for synergistic antibacterial and ablation biofilms', *ACS Appl. Mater. Interfaces*, vol. 12, no. 20, pp. 22479–22491, May 2020, doi: 10.1021/acsami.0c01967.

[6] H.-Z. Lai, W.-Y. Chen, C.-Y. Wu, and Y.-C. Chen, 'Potent antibacterial nanoparticles for pathogenic bacteria', *ACS Appl. Mater. Interfaces*, vol. 7, no. 3, pp. 2046–2054, Jan. 2015, doi: 10.1021/am507919m.

[7] M. J. Hajipour *et al.*, 'Antibacterial properties of nanoparticles', *Trends Biotechnol.*, vol. 30, no. 10, pp. 499–511, Oct. 2012, doi: 10.1016/j.tibtech.2012.06.004.

[8] Y. Yang, Z. Cai, Z. Huang, X. Tang, and X. Zhang, 'Antimicrobial cationic polymers: from structural design to functional control', *Polym. J.*, vol. 50, no. 1, pp. 33–44, Jan. 2018, doi: 10.1038/pj.2017.72.

[9] R. Singh, M. S. Smitha, and S. P. Singh, 'The role of nanotechnology in combating multi-drug resistant bacteria', *J. Nanosci. Nanotechnol.*, vol. 14, no. 7, pp. 4745–4756, Jul. 2014, doi: 10.1166/jnn.2014.9527.

[10] L. Wang, C. Hu, and L. Shao, 'The antimicrobial activity of nanoparticles: present situation and prospects for the future', *Int. J. Nanomedicine*, vol. Volume 12, pp. 1227–1249, Feb. 2017, doi: 10.2147/IJN.S121956.

[11] O. Ozay, A. Akcali, M. T. Otkun, C. Silan, N. Aktas, and N. Sahiner, 'P(4-VP) based nanoparticles and composites with dual action as antimicrobial

materials', *Colloids Surf. B Biointerfaces*, vol. 79, no. 2, pp. 460–466, Sep. 2010, doi: 10.1016/j.colsurfb.2010.05.013.

[12] M. Moritz and M. Geszke-Moritz, 'The newest achievements in synthesis, immobilization and practical applications of antibacterial nanoparticles', *Chem. Eng. J.*, vol. 228, pp. 596–613, Jul. 2013, doi: 10.1016/j.cej.2013.05.046.

[13] C. Vauthier and K. Bouchemal, 'Methods for the preparation and manufacture of polymeric nanoparticles', *Pharm. Res.*, vol. 26, no. 5, pp. 1025–1058, May 2009, doi: 10.1007/s11095-008-9800-3.

[14] A. Zielińska *et al.*, 'Polymeric nanoparticles: production, characterization, toxicology and ecotoxicology', *Molecules*, vol. 25, no. 16, p. 3731, Aug. 2020, doi: 10.3390/molecules25163731.

[15] M. S. Kadayifci *et al.*, 'Core-crosslinking as a pathway to develop inherently antibacterial polymeric micelles', *J. Appl. Polym. Sci.*, vol. 137, no. 8, p. 48393, Feb. 2020, doi: 10.1002/app.48393.

[16] J. P. Rao and K. E. Geckeler, 'Polymer nanoparticles: preparation techniques and size-control parameters', *Prog. Polym. Sci.*, vol. 36, no. 7, pp. 887–913, Jul. 2011, doi: 10.1016/j.progpolymsci.2011.01.001.

[17] C. Pinto Reis, R. J. Neufeld, Ribeiro António J., and F. Veiga, 'Nanoencapsulation I. methods for preparation of drug-loaded polymeric nanoparticles', *Nanomedicine Nanotechnol. Biol. Med.*, vol. 2, no. 1, pp. 8–21, Mar. 2006, doi: 10.1016/j.nano.2005.12.003.

[18] W. Cao *et al.*, 'Facile synthesis of cationic polymer functionalized nanodiamond with high dispersity and antibacterial activity', *J. Mater. Sci.*, vol. 52, no. 4, pp. 1856–1867, Feb. 2017, doi: 10.1007/s10853-016-0475-6.

[19] A. Francesko *et al.*, 'Bacteria-responsive multilayer coatings comprising polycationic nanospheres for bacteria biofilm prevention on urinary catheters', *Acta Biomater.*, vol. 33, pp. 203–212, Mar. 2016, doi: 10.1016/j.actbio.2016.01.020.

[20] N. Beyth, I. Yudovin-Farber, R. Bahir, A. J. Domb, and E. I. Weiss, 'Antibacterial activity of dental composites containing quaternary ammonium polyethylenimine nanoparticles against Streptococcus mutans', *Biomaterials*, vol. 27, no. 21, pp. 3995–4002, Jul. 2006, doi: 10.1016/j.biomaterials.2006.03.003.

[21] M. G. Arafa, H. A. Mousa, and N. N. Afifi, 'Preparation of PLGA-chitosan based nanocarriers for enhancing antibacterial effect of ciprofloxacin in root canal infection', *Drug Deliv.*, vol. 27, no. 1, pp. 26–39, Jan. 2020, doi: 10.1080/10717544.2019.1701140.

[22] M. A. dos Santos Ramos *et al.*, 'Nanotechnological strategies for systemic microbial infections treatment: A review', *Int. J. Pharm.*, vol. 589, p. 119780, Nov. 2020, doi: 10.1016/j.ijpharm.2020.119780.

[23] John E. Bennett, Raphael Dolin, Martin J. Blaser - Mandell, Douglas, and Bennett's 'Principles and practice of infectious diseases' (2020).

[24] T. J. Silhavy, D. Kahne, and S. Walker, 'The bacterial cell envelope', *Cold Spring Harb. Perspect. Biol.*, vol. 2, no. 5, pp. a000414–a000414, May 2010, doi: 10.1101/cshperspect.a000414.

[25] O. Sizar and C. G. Unakal, 'Gram positive bacteria', in *StatPearls*, Treasure Island (FL): StatPearls Publishing, 2022. Accessed: Nov. 15, 2022. [Online]. Available: http://www.ncbi.nlm.nih.gov/books/NBK470553/

[26] J. Oliveira and W. C. Reygaert, 'Gram negative bacteria', in *StatPearls*, Treasure Island (FL): StatPearls Publishing, 2022. Accessed: Nov. 15, 2022. [Online]. Available: http://www.ncbi.nlm.nih.gov/books/NBK538213/

[27] Medical school in UT Southwestern, 'Corbyn Beach - Gram+/- Bacteria'. https://corbynbeach.com/gram-bacteria (accessed Nov. 15, 2022).

[28] F. von Nussbaum, M. Brands, B. Hinzen, S. Weigand, and D. Häbich, 'Antibacterial natural products in medicinal chemistry—exodus or revival?', *Angew. Chem. Int. Ed.*, vol. 45, no. 31, pp. 5072–5129, Aug. 2006, doi: 10.1002/anie.200600350.

[29] J. Cai and R. Liu, 'Introduction to antibacterial biomaterials', *Biomaterials Science*, p. 2, Nov. 2020, doi: 10.1039/d0bm90100h.

[30] J. F. Zachary, 'Mechanisms of microbial infections', in *Pathologic Basis of Veterinary Disease*, Elsevier, 2017, pp. 132-241.e1. doi: 10.1016/B978-0-323-35775-3.00004-7.

[31] E. Palma, B. Tilocca, and P. Roncada, 'Antimicrobial resistance in veterinary medicine: an overview', *Int. J. Mol. Sci.*, vol. 21, no. 6, p. 1914, Mar. 2020, doi: 10.3390/ijms21061914.

[32] L. Wang, C. Hu, and L. Shao, 'The antimicrobial activity of nanoparticles: present situation and prospects for the future', *Int. J. Nanomedicine*, vol. 12, pp. 1227–1249, Feb. 2017, doi: 10.2147/IJN.S121956.

[33] D. L. Rimondini, M. Fini, and R. Giardino, 'The microbial infection of biomaterials: a challenge for clinicians and researchers. a short review', p. 10.

[34] K.-S. Huang, C.-H. Yang, S.-L. Huang, C.-Y. Chen, Y.-Y. Lu, and Y.-S. Lin, 'Recent advances in antimicrobial polymers: a mini-review', *Int. J. Mol. Sci.*, vol. 17, no. 9, p. 1578, Sep. 2016, doi: 10.3390/ijms17091578.

[35] M. Santos *et al.*, 'Recent developments in antimicrobial polymers: a review', *Materials*, vol. 9, no. 7, p. 599, Jul. 2016, doi: 10.3390/ma9070599.

[36] A. Arora and A. Mishra, 'Antibacterial polymers – a mini review', *Mater. Today, Proc.*, vol. 5, no. 9, pp. 17156–17161, 2018, doi: 10.1016/j.matpr.2018.04.124.

[37] M. Nasef, B. Gupta, S. Kamyar, C. Verma, R. rasit ali, and T. Ting, 'Engineered bioactive polymeric surfaces by radiation induced graft

copolymerization: strategies and applications', *Polymers*, vol. 13, p. 3102, Sep. 2021, doi: 10.3390/polym13183102.

[38] A. M. Carmona-Ribeiro and L. D. De Melo Carrasco, 'Cationic antimicrobial polymers and their assemblies', *Int. J. Mol. Sci.*, vol. 14, no. 5, Art. no. 5, May 2013, doi: 10.3390/ijms14059906.

[39] C. N. Galvão, L. M. Sanches, B. I. Mathiazzi, R. T. Ribeiro, D. F. S. Petri, and A. M. Carmona-Ribeiro, 'Antimicrobial coatings from hybrid nanoparticles of biocompatible and antimicrobial polymers', *Int. J. Mol. Sci.*, vol. 19, no. 10, Art. no. 10, Oct. 2018, doi: 10.3390/ijms19102965.

[40] Y. Yang, Z. Cai, Z. Huang, X. Tang, and X. Zhang, 'Antimicrobial cationic polymers: from structural design to functional control', *Polym. J.*, vol. 50, no. 1, pp. 33–44, Jan. 2018, doi: 10.1038/pj.2017.72.

[41] E. F. Palermo and K. Kuroda, 'Chemical structure of cationic groups in amphiphilic polymethacrylates modulates the antimicrobial and hemolytic activities', *Biomacromolecules*, vol. 10, no. 6, pp. 1416–1428, Jun. 2009, doi: 10.1021/bm900044x.

[42] S. Deka, A. Sharma, and P. Kumar, 'Cationic polymers and their self-assembly for antibacterial applications', *Curr. Top. Med. Chem.*, vol. 15, no. 13, pp. 1179–1195, Apr. 2015, doi: 10.2174/1568026615666150330110602.

[43] D. Gokkaya, M. Topuzogullari, T. Arasoglu, K. Trabzonlu, M. M. Ozmen, and S. Abdurrahmanoğlu, 'Antibacterial properties of cationic copolymers as a function of pendant alkyl chain length and degree of quaternization', *Polym. Int.*, vol. 70, no. 6, pp. 829–836, Jun. 2021, doi: 10.1002/pi.6170.

[44] A. C. Engler *et al.*, 'Antimicrobial polycarbonates: investigating the impact of balancing charge and hydrophobicity using a same-centered polymer approach', *Biomacromolecules*, vol. 14, no. 12, pp. 4331–4339, Dec. 2013, doi: 10.1021/bm401248t.

[45] B. Dizman, M. O. Elasri, and L. J. Mathias, 'Synthesis and antimicrobial activities of new water-soluble bis-quaternary ammonium methacrylate polymers', *J. Appl. Polym. Sci.*, vol. 94, no. 2, pp. 635–642, Oct. 2004, doi: 10.1002/app.20872.

[46] G. Lu, D. Wu, and R. Fu, 'Studies on the synthesis and antibacterial activities of polymeric quaternary ammonium salts from dimethylaminoethyl methacrylate', *React. Funct. Polym.*, vol. 67, no. 4, pp. 355–366, Apr. 2007, doi: 10.1016/j.reactfunctpolym.2007.01.008.

[47] K. Mavronasou *et al.*, 'Poly(vinyl pyridine) and its quaternized derivatives: understanding their solvation and solid-state properties', *Polymers*, vol. 14, no. 4, Art. no. 4, Jan. 2022, doi: 10.3390/polym14040804.

[48] Z. Iatridi and C. Tsitsilianis, 'Water-soluble stimuli responsive star-shaped segmented macromolecules', *Polymers*, vol. 3, no. 4, Art. no. 4, Dec. 2011, doi: 10.3390/polym3041911.

[49] L. Cen, K. G. Neoh, and E. T. Kang, 'Antibacterial activity of cloth functionalized with N-alkylated poly(4-vinylpyridine)', *J. Biomed. Mater. Res. A*, vol. 71A, no. 1, pp. 70–80, 2004, doi: 10.1002/jbm.a.30125.

[50] F. Bucatariu *et al.*, 'An overview on composite sorbents based on polyelectrolytes used in advanced wastewater treatment', *Polymers*, vol. 13, no. 22, Art. no. 22, Jan. 2021, doi: 10.3390/polym13223963.

[51] E. N. Durmaz, S. Sahin, E. Virga, S. de Beer, L. C. P. M. de Smet, and W. M. de Vos, 'Polyelectrolytes as building blocks for next-generation membranes with advanced functionalities', *ACS Appl. Polym. Mater.*, vol. 3, no. 9, pp. 4347–4374, Sep. 2021, doi: 10.1021/acsapm.1c00654.

[52] A. V. Ambade, B. S. Sandanaraj, A. Klaikherd, and S. Thayumanavan, 'Fluorescent polyelectrolytes as protein sensors', *Polym. Int.*, vol. 56, no. 4, pp. 474–481, 2007, doi: 10.1002/pi.2185.

[53] H. Mortazavian, L. Foster, R. Bhat, S. Patel, and K. Kuroda, 'Decoupling the functional roles of cationic and hydrophobic groups in the antimicrobial and hemolytic activities of methacrylate random copolymers', *Biomacromolecules*, vol. 19, Oct. 2018, doi: 10.1021/acs.biomac.8b01256.

[54] Z. Farrokhi, A. Ayati, M. Kanvisi, and M. Sillanpää, 'Recent advance in antibacterial activity of nanoparticles contained polyurethane', *J. Appl. Polym. Sci.*, vol. 136, no. 4, p. 46997, Jan. 2019, doi: 10.1002/app.46997.

[55] M. J. Hajipour *et al.*, 'Antibacterial properties of nanoparticles', *Trends Biotechnol.*, vol. 30, no. 10, pp. 499–511, Oct. 2012, doi: 10.1016/j.tibtech.2012.06.004.

[56] M. Barani *et al.*, 'Nanomaterials in the management of gram-negative bacterial infections', *Nanomaterials*, vol. 11, no. 10, p. 2535, Sep. 2021, doi: 10.3390/nano11102535.

[57] N. E. Eleraky, A. Allam, S. B. Hassan, and M. M. Omar, 'Nanomedicine fight against antibacterial resistance: an overview of the recent pharmaceutical innovations', *Pharmaceutics*, vol. 12, no. 2, p. 142, Feb. 2020, doi: 10.3390/pharmaceutics12020142.

[58] J. R. Morones *et al.*, 'The bactericidal effect of silver nanoparticles', *Nanotechnology*, vol. 16, no. 10, pp. 2346–2353, Oct. 2005, doi: 10.1088/0957-4484/16/10/059.

[59] L. Qi, Z. Xu, X. Jiang, C. Hu, and X. Zou, 'Preparation and antibacterial activity of chitosan nanoparticles', *Carbohydr. Res.*, vol. 339, no. 16, pp. 2693–2700, Nov. 2004, doi: 10.1016/j.carres.2004.09.007.

[60] H. Barani, M. Montazer, T. Toliyat, and N. Samadi, 'Synthesis of Ag-liposome nano composites', *J. Liposome Res.*, vol. 20, no. 4, pp. 323–329, Dec. 2010, doi: 10.3109/08982100903544177.

[61] S. Kang, M. Herzberg, D. F. Rodrigues, and M. Elimelech, 'Antibacterial effects of carbon nanotubes: size does matter!', *Langmuir*, vol. 24, no. 13, pp. 6409–6413, Jul. 2008, doi: 10.1021/la800951v.

[62] X. Zhao, ‘Antibacterial bioactive materials’, in *Bioactive Materials in Medicine*, Elsevier, 2011, pp. 97–123. doi: 10.1533/9780857092939.2.97.

[63] A. A. Ashkarran, M. Ghavami, H. Aghaverdi, P. Stroeve, and M. Mahmoudi, ‘Bacterial effects and protein corona evaluations: crucial ignored factors in the prediction of bio-efficacy of various forms of silver nanoparticles’, *Chem. Res. Toxicol.*, vol. 25, no. 6, pp. 1231–1242, Jun. 2012, doi: 10.1021/tx300083s.

[64] M. R. W. BROWN, D. G. ALLISON, and P. GILBERT, ‘Resistance of bacterial biofilms to antibiotics a growth-rate related effect?’, *J. Antimicrob. Chemother.*, vol. 22, no. 6, pp. 777–780, Dec. 1988, doi: 10.1093/jac/22.6.777.

[65] F. Andrade, D. Rafael, M. Videira, D. Ferreira, A. Sosnik, and B. Sarmento, ‘Nanotechnology and pulmonary delivery to overcome resistance in infectious diseases’, *Adv. Drug Deliv. Rev.*, vol. 65, no. 13, pp. 1816–1827, Nov. 2013, doi: 10.1016/j.addr.2013.07.020.

[66] G. Qi, L. Li, F. Yu, and H. Wang, ‘Vancomycin-modified mesoporous silica nanoparticles for selective recognition and killing of pathogenic gram-positive bacteria over macrophage-like cells’, *ACS Appl. Mater. Interfaces*, vol. 5, no. 21, pp. 10874–10881, Nov. 2013, doi: 10.1021/am403940d.

[67] A. Rai, M. Comune, and L. Ferreira, ‘Nanoparticle-based drug delivery systems: promising approaches against bacterial infections’, in *Antibacterial Drug Discovery to Combat MDR: Natural Compounds, Nanotechnology and Novel Synthetic Sources*, I. Ahmad, S. Ahmad, and K. P. Rumbaugh, Eds. Singapore: Springer, 2019, pp. 605–633. doi: 10.1007/978-981-13-9871-1_27.

[68] M. Raffi *et al.*, ‘Investigations into the antibacterial behavior of copper nanoparticles against Escherichia coli’, *Ann. Microbiol.*, vol. 60, no. 1, pp. 75–80, Mar. 2010, doi: 10.1007/s13213-010-0015-6.

[69] A. b. g. Lansdown, ‘Silver I: its antibacterial properties and mechanism of action’, *J. Wound Care*, vol. 11, no. 4, pp. 125–130, Apr. 2002, doi: 10.12968/jowc.2002.11.4.26389.

[70] S. Li *et al.*, ‘Antibacterial hydrogels’, *Adv. Sci.*, vol. 5, no. 5, p. 1700527, 2018, doi: 10.1002/advs.201700527.

[71] S. S. N. Fernando, T. D. C. P. Gunasekara, and J. Holton, ‘Antimicrobial Nanoparticles: applications and mechanisms of action’, 2018, doi: 10.4038/sljid.v8i1.8167.

[72] I. Sondi and B. Salopek-Sondi, ‘Silver nanoparticles as antimicrobial agent: a case study on *E. coli* as a model for Gram-negative bacteria’, *J. Colloid Interface Sci.*, vol. 275, no. 1, pp. 177–182, Jul. 2004, doi: 10.1016/j.jcis.2004.02.012.

[73] M. Rai, A. Yadav, and A. Gade, ‘Silver nanoparticles as a new generation of antimicrobials’, *Biotechnol. Adv.*, vol. 27, no. 1, pp. 76–83, Jan. 2009, doi: 10.1016/j.biotechadv.2008.09.002.

[74] Q. L. Feng, J. Wu, G. Q. Chen, F. Z. Cui, T. N. Kim, and J. O. Kim, 'A mechanistic study of the antibacterial effect of silver ions on *Escherichia coli* and *Staphylococcus aureus*', *J. Biomed. Mater. Res.*, vol. 52, no. 4, pp. 662–668, 2000, doi: 10.1002/1097-4636(20001215)52:4<662:AID-JBM10>3.0.CO;2-3.

[75] S. Shrivastava, T. Bera, A. Roy, G. Singh, P. Ramachandrarao, and D. Dash, 'Characterization of enhanced antibacterial effects of novel silver nanoparticles', *Nanotechnology*, vol. 18, no. 22, p. 225103, May 2007, doi: 10.1088/0957-4484/18/22/225103.

[76] A. Ivask *et al.*, 'Toxicity mechanisms in *Escherichia coli* vary for silver nanoparticles and differ from ionic silver', *ACS Nano*, vol. 8, no. 1, pp. 374–386, Jan. 2014, doi: 10.1021/nn4044047.

[77] Y. Matsumura, K. Yoshikata, S. Kunisaki, and T. Tsuchido, 'Mode of Bactericidal action of silver zeolite and its comparison with that of silver nitrate', *Appl. Environ. Microbiol.*, vol. 69, no. 7, pp. 4278–4281, Jul. 2003, doi: 10.1128/AEM.69.7.4278-4281.2003.

[78] Y. Cui, Y. Zhao, Y. Tian, W. Zhang, X. Lü, and X. Jiang, 'The molecular mechanism of action of bactericidal gold nanoparticles on *Escherichia coli*', *Biomaterials*, vol. 33, no. 7, pp. 2327–2333, Mar. 2012, doi: 10.1016/j.biomaterials.2011.11.057.

[79] R. A. Festa and D. J. Thiele, 'Copper: an essential metal in biology', *Curr. Biol.*, vol. 21, no. 21, pp. R877–R883, Nov. 2011, doi: 10.1016/j.cub.2011.09.040.

[80] C. Ariöz and P. Wittung-Stafshede, 'Folding of copper proteins: role of the metal?', *Q. Rev. Biophys.*, vol. 51, p. e4, ed 2018, doi: 10.1017/S0033583518000021.

[81] Y. Wu, W. Wu, W. Zhao, and X. Lan, 'Revealing the antibacterial mechanism of copper surfaces with controllable microstructures', *Surf. Coat. Technol.*, vol. 395, p. 125911, Aug. 2020, doi: 10.1016/j.surfcoat.2020.125911.

[82] M. Vincent, R. e. Duval, P. Hartemann, and M. Engels-Deutsch, 'Contact killing and antimicrobial properties of copper', *J. Appl. Microbiol.*, vol. 124, no. 5, pp. 1032–1046, 2018, doi: 10.1111/jam.13681.

[83] A. A. Menazea and M. K. Ahmed, 'Nanosecond laser ablation assisted the enhancement of antibacterial activity of copper oxide nano particles embedded though Polyethylene Oxide/Polyvinyl pyrrolidone blend matrix', *Radiat. Phys. Chem.*, vol. 174, p. 108911, Sep. 2020, doi: 10.1016/j.radphyschem.2020.108911.

[84] A. K. Chatterjee, R. Chakraborty, and T. Basu, 'Mechanism of antibacterial activity of copper nanoparticles', *Nanotechnology*, vol. 25, no. 13, p. 135101, Feb. 2014, doi: 10.1088/0957-4484/25/13/135101.

[85] M. Rai, S. D. Deshmukh, A. P. Ingle, I. R. Gupta, M. Galdiero, and S. Galdiero, 'Metal nanoparticles: The protective nanoshield against virus infection', *Crit. Rev. Microbiol.*, vol. 42, no. 1, pp. 46–56, Jan. 2016, doi: 10.3109/1040841X.2013.879849.

[86] J. Liu and R. H. Hurt, 'Ion release kinetics and particle persistence in aqueous nano-silver colloids', *Environ. Sci. Technol.*, vol. 44, no. 6, pp. 2169–2175, Mar. 2010, doi: 10.1021/es9035557.

[87] S. Zhang, C. Du, Z. Wang, X. Han, K. Zhang, and L. Liu, 'Reduced cytotoxicity of silver ions to mammalian cells at high concentration due to the formation of silver chloride', *Toxicol. In Vitro*, vol. 27, no. 2, pp. 739–744, Mar. 2013, doi: 10.1016/j.tiv.2012.12.003.

[88] S. H. Lee and B.-H. Jun, 'Silver nanoparticles: synthesis and application for nanomedicine', *Int. J. Mol. Sci.*, vol. 20, no. 4, Art. no. 4, Jan. 2019, doi: 10.3390/ijms20040865.

[89] M. Godoy-Gallardo *et al.*, 'Antibacterial approaches in tissue engineering using metal ions and nanoparticles: From mechanisms to applications', *Bioact. Mater.*, vol. 6, no. 12, pp. 4470–4490, Dec. 2021, doi: 10.1016/j.bioactmat.2021.04.033.

[90] H. Spieser, A. Jardin, D. Deganello, D. Gethin, J. Bras, and A. Denneulin, 'Rheology of cellulose nanofibrils and silver nanowires for the development of screen-printed antibacterial surfaces', *J. Mater. Sci.*, vol. 56, no. 21, pp. 12524–12538, Jul. 2021, doi: 10.1007/s10853-021-06082-y.

[91] A. K. Suresh *et al.*, 'Silver nanocrystallites: biofabrication using Shewanella oneidensis, and an evaluation of their comparative toxicity on gram-negative and gram-positive bacteria', *Environ. Sci. Technol.*, vol. 44, no. 13, pp. 5210–5215, Jul. 2010, doi: 10.1021/es903684r.

[92] M. P. Patil and G.-D. Kim, 'Eco-friendly approach for nanoparticles synthesis and mechanism behind antibacterial activity of silver and anticancer activity of gold nanoparticles', *Appl. Microbiol. Biotechnol.*, vol. 101, no. 1, pp. 79–92, Jan. 2017, doi: 10.1007/s00253-016-8012-8.

[93] O. Choi, K. K. Deng, N.-J. Kim, L. Ross, R. Y. Surampalli, and Z. Hu, 'The inhibitory effects of silver nanoparticles, silver ions, and silver chloride colloids on microbial growth', *Water Res.*, vol. 42, no. 12, pp. 3066–3074, Jun. 2008, doi: 10.1016/j.watres.2008.02.021.

[94] Y.-M. Long *et al.*, 'Surface ligand controls silver ion release of nanosilver and its antibacterial activity against *Escherichia coli*', *Int. J. Nanomedicine*, vol. 12, pp. 3193–3206, Apr. 2017, doi: 10.2147/IJN.S132327.

[95] Y.-F. Li and C. Chen, 'Fate and toxicity of metallic and metal-containing nanoparticles for biomedical applications', *Small*, vol. 7, no. 21, pp. 2965–2980, 2011, doi: 10.1002/smll.201101059.

[96] T. Safarov, B. Kiran, M. Bagirova, A. M. Allahverdiyev, and E. S. Abamor, 'An overview of nanotechnology-based treatment approaches against *Helicobacter Pylori*', *Expert Rev. Anti Infect. Ther.*, vol. 17, no. 10, pp. 829–840, Oct. 2019, doi: 10.1080/14787210.2019.1677464.

[97] G. E. Valenti, S. Alfei, D. Caviglia, C. Domenicotti, and B. Marengo, 'Antimicrobial peptides and cationic nanoparticles: a broad-spectrum weapon to fight multi-drug resistance not only in bacteria', *Int. J. Mol. Sci.*, vol. 23, no. 11, p. 6108, May 2022, doi: 10.3390/ijms23116108.

[98] J. Hoque *et al.*, 'Selective and broad spectrum amphiphilic small molecules to combat bacterial resistance and eradicate biofilms', *Chem. Commun.*, vol. 51, no. 71, pp. 13670–13673, Aug. 2015, doi: 10.1039/C5CC05159B.

[99] Y. Zhu, C. Xu, N. Zhang, X. Ding, B. Yu, and F.-J. Xu, 'Polycationic synergistic antibacterial agents with multiple functional components for efficient anti-infective therapy', *Adv. Funct. Mater.*, vol. 28, no. 14, p. 1706709, 2018, doi: 10.1002/adfm.201706709.

[100] K. A. Brogden, 'Antimicrobial peptides: pore formers or metabolic inhibitors in bacteria?', *Nat. Rev. Microbiol.*, vol. 3, no. 3, Art. no. 3, Mar. 2005, doi: 10.1038/nrmicro1098.

[101] S. J. Lam, E. H. H. Wong, C. Boyer, and G. G. Qiao, 'Antimicrobial polymeric nanoparticles', *Prog. Polym. Sci.*, vol. 76, pp. 40–64, Jan. 2018, doi: 10.1016/j.progpolymsci.2017.07.007.

[102] O. I. Parisi, L. Scrivano, M. S. Sinicropi, and F. Puoci, 'Polymeric nanoparticle constructs as devices for antibacterial therapy', *Curr. Opin. Pharmacol.*, vol. 36, pp. 72–77, Oct. 2017, doi: 10.1016/j.coph.2017.08.004.

[103] L. Zhai, Z. Zhang, Y. Zhao, and Y. Tang, 'Efficient antibacterial performance and effect of structure on property based on cationic conjugated polymers', *Macromolecules*, vol. 51, no. 18, pp. 7239–7247, Sep. 2018, doi: 10.1021/acs.macromol.8b01530.

[104] Q. M. Zhang and M. J. Serpe, 'Synthesis, characterization, and antibacterial properties of a hydroxyapatite adhesive block copolymer', *Macromolecules*, vol. 47, no. 22, pp. 8018–8025, Nov. 2014, doi: 10.1021/ma501997x.

[105] Y. Jiang *et al.*, 'Acid-activated antimicrobial random copolymers: a mechanism-guided design of antimicrobial peptide mimics', *Macromolecules*, vol. 46, no. 10, pp. 3959–3964, May 2013, doi: 10.1021/ma400484b.

[106] M. Topuzoğullari, 'Effect of polyelectrolyte complex formation on the antibacterial activity of copolymer of alkylated 4-vinylpyridine', *Turk. J. Chem.*, vol. 44, no. 3, pp. 634–646, Jun. 2020, doi: 10.3906/kim-1909-95.

[107] M. Topuzogullari, 'Microwave assisted quaternization of poly(4-vinylpyridine) with 1-bromohexane', *J. Polym. Res.*, vol. 25, no. 8, p. 188, Jul. 2018, doi: 10.1007/s10965-018-1581-8.

[108] M. do Socorro Costa *et al.*, 'Evaluation of the antibacterial and inhibitory activity of NorA and MepA efflux pumps from Staphylococcus aureus by diosgenin', *Life Sci.*, vol. 308, p. 120978, Nov. 2022, doi: 10.1016/j.lfs.2022.120978.

[109] J. D. Unciti-Broceta, V. Cano-Cortés, P. Altea-Manzano, S. Pernagallo, J. J. Díaz-Mochón, and R. M. Sánchez-Martín, 'Number of nanoparticles per cell through a spectrophotometric method - a key parameter to assess nanoparticle-based cellular assays', *Sci. Rep.*, vol. 5, no. 1, Art. no. 1, May 2015, doi: 10.1038/srep10091.

[110] O. K. Gulevskyy, N. M. Moisieieva, O. L. Gorina, and O. S. Sidorenko, ‘Preincubation of L929 line fibroblasts with synthetic Leu-Enkephalin TYR-D-ALA-GLY-PHE-LEU-ARG preserves their proliferative potential under cold stress’, *Cytol. Genet.*, vol. 56, no. 4, pp. 343–350, Aug. 2022, doi: 10.3103/S0095452722040053.

[111] H. Shiraishi and A. Toyoda, ‘The use of a 3-(4,5-dimethylthiazol-2-yl)-2,5-diphenyl tetrazolium bromide–based colorimetric assay in the viability analysis of the filamentous cyanobacterium Arthrospira platensis’, *Biosci. Biotechnol. Biochem.*, vol. 85, no. 3, pp. 739–742, Mar. 2021, doi: 10.1093/bbb/zbaa050.

[112] S. Rekha and E. I. Anila, ‘In vitro cytotoxicity studies of surface modified CaS nanoparticles on L929 cell lines using MTT assay’, *Mater. Lett.*, vol. 236, pp. 637–639, Feb. 2019, doi: 10.1016/j.matlet.2018.11.009.

[113] G. Singh, K. Tanurajvir, K. Ravinder, and A. Kaur, ‘Recent biomedical applications and patents on biodegradable polymer-PLGA’, *Int. J. Pharmacol. Pharm. Sci.*, vol. 1, pp. 30–42, Jan. 2014.

[114] M. Dandamudi *et al.*, ‘Chitosan-coated PLGA nanoparticles encapsulating triamcinolone acetonide as a potential candidate for sustained ocular drug delivery’, *Pharmaceutics*, vol. 13, no. 10, Art. no. 10, Oct. 2021, doi: 10.3390/pharmaceutics13101590.

[115] S. Y. Lee, J. S. Koo, M. Yang, and H.-J. Cho, ‘Application of temporary agglomeration of chitosan-coated nanoparticles for the treatment of lung metastasis of melanoma’, *J. Colloid Interface Sci.*, vol. 544, pp. 266–275, May 2019, doi: 10.1016/j.jcis.2019.02.092.

[116] S. A. AlQahtani, G. I. Harisa, A. H. Alomrani, F. K. Alanazi, and M. M. Badran, ‘Improved pharmacokinetic and biodistribution of 5-fluorouracil loaded biomimetic nanoerythrocytes decorated nanocarriers for liver cancer treatment’, *Colloids Surf. B Biointerfaces*, vol. 197, p. 111380, Jan. 2021, doi: 10.1016/j.colsurfb.2020.111380.

PUBLICATIONS FROM THE THESIS

Conference Papers

Alhamvi S., Akmayan İ., Özbek T., Topuzoğulları M., " Synthesis and Characterization of Inherently Antibacterial Cationic Nanoparticles " 16th Nanoscience and Nanotechnology Conference, NanoTR16, Middle East Technical University, Ankara, Turkey, 06.09.2022.

Project

“Kendiliğinden Antibakteriyel Polimerik Malzemelerin Geliştirilmesi”, The Scientific Research Projects Coordination Unit of Yildiz Technical University, Project No: FCD-2022-4900, Principal Investigator: Assoc. Prof. Dr. Murat Topuzoğulları, 2022-2024.

Scolarship

"Kendiliğinden Antibakteriyel Katyonik Nanopartiküllerin Sentezi ve Karakterizasyonu" TÜBİTAK-2210C Domestic Priority Areas Graduate Scholarship -2021/2.